

1 **Title page**

2

3 **The spectrum of *IDH*- and *H3*-wildtype high-grade glioma subgroups occurring across teenage and**  
4 **young adult patient populations**

5

6 **Authors:**

7

8 Rita Pereira<sup>1\*</sup>, Alan Mackay<sup>1\*</sup>, Yura Grabovska<sup>1\*</sup>, Amelia Bradley<sup>2</sup>, Tabitha Bloom<sup>2</sup>, James Nicoll<sup>2</sup>,  
9 Delphine Boche<sup>2</sup>, John Procter<sup>3</sup>, Mellissa Maybury<sup>4,5</sup>, Johanna Schagen<sup>5</sup>, Liam Walker<sup>6,7</sup>, Federico Roncaroli<sup>6,7</sup>,  
10 Konstantina Karabatsou<sup>8</sup>, Olumide Ogunbiyi<sup>9</sup>, Thijs van Dalen<sup>10</sup>, Jai Sidpra<sup>17</sup>, Sabrina Rossi<sup>11</sup>, Evelina Miele<sup>12</sup>,  
11 David S. Ziegler<sup>13,14,15</sup>, Zhifeng Shi<sup>16</sup>, Thomas S. Jacques<sup>7</sup>, Darren Hargrave<sup>17</sup>, Bassel Zebian<sup>18</sup>, Cristina Bleil<sup>18</sup>,  
12 Joseph Yates<sup>19</sup>, Emma Norton<sup>19</sup>, Henry Mandeville<sup>20</sup>, Antonia Creak<sup>21</sup>, Liam Welsh<sup>21</sup>, Lynley Marshall<sup>22,20,23</sup>,  
13 Fernando Carceller<sup>20</sup>, Sucheta J. Vaidya<sup>20</sup>, Zita Reisz<sup>24</sup>, Safa Al-Sarraj<sup>24</sup>, Angela Mastronuzzi<sup>25</sup>, Andrea Carai<sup>26</sup>,  
14 Maria Vinci<sup>27</sup>, Kathreena M. Kurian<sup>28</sup>, Ho-keung Ng<sup>29</sup>, Sebastian Brandner<sup>30</sup>, Chris Jones<sup>1\*</sup>, Matthew  
15 Clarke<sup>1,30\*</sup>

16

17 \*Indicates that these authors contributed equally to the work.

18

19 **Affiliations:**

20

21

22

23

24

25

26

27

28

29

30

31

32

33

34

35

36

37

38

39

40

1. Division of Molecular Pathology, Institute of Cancer Research, United Kingdom
2. Clinical Neurosciences, Clinical and Experimental Sciences, Faculty of Medicine, University of Southampton, Southampton, United Kingdom
3. Neuropathology and Pathology Research, Royal Preston Hospital
4. Oncology Services Group, Queensland Children's Hospital, Brisbane, Queensland, Australia.
5. Child Health Research Centre, The University of Queensland, Brisbane, Queensland, Australia
6. Department of Cellular Pathology, Northern Care Alliance, Salford, United Kingdom.
7. Geoffrey Jefferson Brain Research Centre, Division of Neuroscience, School of Biology, University of Manchester, United Kingdom.
8. Department of Neurosurgery, Manchester Centre of Clinical Neuroscience, Northern Care Alliance
9. Neuropathology Department, Great Ormond Street Hospital for Children NHS Foundation Trust, United Kingdom
10. Neurosurgery Department, National Hospital for Neurology and Neurosurgery, UCLH, United Kingdom
11. Sabrina Rossi. Pathology Unit, Bambino Gesù Children's Hospital IRCCS, Rome, Italy
12. Evelina Miele. Pediatric Onco-Haematology, Cell Therapy, Gene Therapies and Hematopoietic Transplant, Bambino Gesù Children's Hospital-IRCCS, Rome, Italy
13. Children's Cancer Institute, Lowy Cancer Centre, UNSW Sydney, Kensington, NSW, Australia
14. School of Clinical Medicine, UNSW Medicine & Health, UNSW Sydney, Kensington, NSW, Australia
15. Kids Cancer Centre, Sydney Children's Hospital, Randwick, NSW, Australia
16. Neurosurgery, Fudan University

- 41 17. Paediatric Neuro Oncology, UCL Great Ormond Street Institute of Child Health, London, UK  
42 18. Neurosurgery Department, King's College Hospital, London, United Kingdom  
43 19. Department of Cellular Pathology, University Hospital Southampton NHS Trust, Southampton, United  
44 Kingdom  
45 20. Department of Paediatric and Teenager & Young Adult Neuro-Oncology, The Royal Marsden Hospital  
46 NHS Foundation Trust, United Kingdom; Division of Clinical Studies, The Institute of Cancer  
47 Research, London, United Kingdom.  
48 21. Department of Adult Neuro-Oncology, The Royal Marsden Hospital NHS Foundation Trust, United  
49 Kingdom; Division of Clinical Studies, The Institute of Cancer Research, London, United Kingdom.  
50 22. Paediatric and Adolescent Oncology Drug Development Unit, The Royal Marsden NHS Foundation  
51 Trust, UK  
52 23. Division of Clinical Studies, The Institute of Cancer Research, UK  
53 24. Neuropathology Department, King's College Hospital, United Kingdom  
54 25. Pediatric Onco-Hematology, Cell Therapy, Gene Therapies and Hematopoietic Transplant, Bambino  
55 Gesù Children's Hospital - IRCCS, Rome, Italy  
56 26. Neurosurgery Unit, Bambino Gesù Children's Hospital – IRCCS, Rome, Italy  
57 27. Mara. Paediatric Cancer Genetics and Epigenetics Research Unit, Bambino Gesù Children's Hospital-  
58 IRCCS, Rome, Italy  
59 28. University of Bristol Brain Tumour Research Centre, Neuropathology, Southmead Hospital, Bristol,  
60 United Kingdom  
61 29. Chinese University of Hong Kong, Hong Kong  
62 30. Division of Neuropathology, The National Hospital for Neurology and Neurosurgery, University  
63 College London Hospitals NHS Foundation Trust, and Queen Square Institute of Neurology, United  
64 Kingdom  
65

66 **Corresponding author:**

67 Dr Matthew Clarke

68 Division of Molecular Pathology

69 Institute of Cancer Research

70 15 Cotswold Road

71 Sutton

72 London

73 SM2 5NG

74 Email: matthew.clarke01@icr.ac.uk  
75

76 **Conflicts of interest**

77 No conflicts of interest to declare  
78

79 **Other notes**

80 Word count abstract: 374

81 Word count text: 8225  
82 Word count references: 1520  
83 Word count figure and table legends: 1866  
84 Number of figures: 6  
85 Supplementary material: 6 supplementary figures, 4 supplementary tables

86

87 **Statement of translational relevance**

88

89 High-grade gliomas (HGG) in teenagers and young adults (TYA) are an understudied group of tumours.  
90 Through national and international collaboration, we have gathered a large series of 207 cases, for the purpose  
91 of molecular characterisation using DNA methylation profiling, whole exome sequencing and fusion panel  
92 sequencing, alongside neuropathological review. We integrate histopathology, genetic and epigenetic profiling  
93 to present the spectrum of different subtypes of HGG which occur in the TYA population. We identify that  
94 HGGs occurring in TYAs comprise of methylation subgroups which occur in paediatric and adult age groups,  
95 but also novel, poorly defined methylation classes which this study helps to characterise. The study highlights  
96 mutational landscapes which may be targetable with immune checkpoint, MAPK-pathway and *PDGFRA*  
97 inhibitors. Incidences of tumour predisposition syndromes (including constitutional mismatch repair disorder  
98 (CMMRD)) are identified in the cohort, and we also identify tumours that have developed on a background of  
99 previous treatment for childhood cancers. These data also highlight the value of undertaking DNA methylation  
100 profiling and whole exome/panel sequencing on each HGG occurring in the TYA age group to accurately  
101 diagnose and characterise these complex tumours.

102

103

104

105

106

107

108

109

110

111

112

113

114

115

116

117

118

119

120

121

122  
123  
124  
125  
126  
127  
128  
129  
130  
131  
132  
133  
134  
135  
136  
137  
138  
139  
140  
141  
142  
143  
144  
145  
146  
147  
148  
149  
150  
151  
152  
153  
154  
155  
156  
157  
158  
159

## **Abstract**

### **Background**

High-grade gliomas (HGG) occur in any central nervous system (CNS) location and at any age. HGGs in teenagers/young adults (TYA) are understudied. This project aimed to characterise these tumours to support accurate stratification of patients.

### **Methods**

207 histone/IDH-wildtype tumours from patients aged 13–30 years were collected. DNA methylation profiling (Illumina EPIC BeadArrays, brain tumour classifier (MNPv12.8 R package)) classified cases against reference cohorts of HGG. Calibrated scores guided characterisation workflows (RNA-based ArcherDx fusion panel (n=92), whole exome sequencing (WES) (n=107), histological review).

### **Results**

53.4% (n=86) matched as paediatric-type subgroups (pedHGG\_RTK1A/B/C (31.7%, n=51 *PDGFRA*, *CDKN2A/B*, *SETD2*, *NF1* alterations), pedHGG\_MYCN (8.1%, n=13, *MYCN/ID2* amplifications), and pedHGG\_RTK2A/B (7.5%, n=12, *TP53*, *BCOR*, *ATRX*, *EGFR* alterations)). 18.0% (n=29) classified as adult-type subgroups (GBM\_MES (15.5%, n=25, enriched for *RBI*, *PTEN*, *NF1* alterations) and GBM\_RTK1/2 (2.5%, n=4, *CDK4* amplifications)). 23 cases (14.7%) classified as novel, poorly-characterised subgroups with distinct methylation profiles and molecular features (pedHGG\_A/B (n=10 6.2%), HGG\_E (n=6 3.7%), HGG\_B (n=2 1.0%), GBM\_CBM (n=5 3.1%)) with variable histological morphology. 8 cases (5.1%) showed hypermutator phenotypes, enriched in HGG\_E, one of which was associated with constitutional mismatch repair deficiency (CMMRD), and their sibling who was diagnosed with the same syndrome, was diagnosed with a tumour which classified as a pedHGG\_RTK1B. HGGs which have developed on a background of previous treatment for a childhood cancer are detected in the TYA population, classifying most frequently as pedHGG\_RTK1B, and contributing to the poor prognosis of this subgroup. Age-distribution/molecular profile comparisons using publicly available methylation/sequencing data (and from local diagnostic cohorts) for HGG\_B (n=19), GBM\_CBM (n=35) and GBM\_MES\_ATYP (n=102), irrespective of age, show that HGG\_B is a TYA-specific subgroup (median age 29 years) and that GBM\_CBM and GBM\_MES\_ATYP show a peak of distribution in the TYA population, but also have a wider age distribution (median age 35.7 and 50.5 years respectively) with the latter showing distinct differences in copy number profiles compared to older adults in the same subgroup, and containing fewer chr7 gains, chr10 losses, more *CDKN2A/B* deletions and *MET* amplifications, and a worse survival compared with adult-specific GBM\_MES\_TYP.

### **Conclusion**

160 TYA HGGs comprise novel methylation subgroups with distinct methylation and molecular profiles. Accurate  
161 stratification of these patients will open opportunities to more effective treatments including immune check  
162 point, MAPK-pathway and *PDGFRA* inhibitors.

163

164

## 165 **Introduction**

166

167 High-grade gliomas (HGG) comprise different subgroups of aggressive central nervous system (CNS) tumours  
168 in both adults and children including infants (1,2). They can occur in any CNS location (3,4) within the cranio-  
169 spinal axis and have a poor prognosis (20.8% 5-year survival for those diagnosed between 0-19 years and 21.9%  
170 for patients aged 20-44 years) (3,5). Outcomes are considerably better than older adults with patients aged 45-54  
171 and 55-64 years having a 5-year survival of 9.3% and 5.9% respectively, suggesting that underlying biology  
172 may differ (3). It remains a significant clinical and therapeutic challenge to understand more about the  
173 development, characteristics and evolution of these tumours to advance therapeutic interventions and improve  
174 survival (6,7).

175

176 DNA methylation profiling and the development of the Molecular Neuropathology (MNP) brain tumour  
177 classifier have transformed diagnostic practice (8,9), providing a molecular tool supporting delivery of accurate  
178 diagnoses for challenging cases. Copy number profiles and prognostic information can be gained (9), and it  
179 provides opportunities to discover and characterise new tumour entities (8,9) for more accurate patient  
180 stratification (10,11).

181

182 The 5<sup>th</sup> edition of the World Health Organisation (WHO) classification of tumours of the CNS now recognises  
183 that high- and low-grade diffuse glial tumours occurring in adults and children comprise distinct entities with  
184 distinctive molecular profiles (12); histone-mutant CNS tumours (diffuse midline glioma, H3 K27-altered,  
185 diffuse hemispheric glioma, H3 G34-mutant) are considered paediatric-type HGGs (12,13). The WHO  
186 classification also recognises the newly defined paediatric entities including the infant-type hemispheric glioma  
187 (IHG), seen predominantly in the infant population, and characterised by distinct methylation profiles and RTK  
188 fusions (1,2).

189

190 Approximately 60% of CNS tumours diagnosed in teenagers and young adults (TYA) each year in the UK will  
191 be a glial tumour (14), representing the fourth most frequent cancer type occurring in patients aged 15–24 years  
192 (12). They account for 60% of cancer-related deaths in this age range (14). This group denotes an understudied  
193 set of tumours with very limited published clinical, pathological and molecular data. No distinct HGG  
194 subgroups are recognised as TYA-specific according to the WHO classification (12). Studies have explored a  
195 variety of molecular-based techniques (immunohistochemistry, targeted/next generation sequencing, whole  
196 exome sequencing and much less frequently epigenetic profiling) and show that a proportion of TYA HGGs can  
197 be classified into well-recognised HGG entities including diffuse midline gliomas, H3 K27-altered, diffuse  
198 hemispheric glioma, H3 G34-mutant, and IDH-mutant HGGs (15,16). However, other tumours remained  
199 unclassifiable (15). A meta- analysis of >1000 paediatric HGG and diffuse midline gliomas (DMGs), including

200 patients aged up to 35 years, identified diverse clinical and biological subgroups characterised by different  
201 somatic mutations (16), and showed that survival of TYA HGGs was significantly better compared to older  
202 adults and H3-mutant groups (16), suggesting that novel entities of HGG with differing underlying biology  
203 exist.

204

205 Gross total resection (GTR) is the mainstem HGG treatment, including for TYA patients. Given their infiltrative  
206 nature, residual and radiologically undetectable tumour frequently remains, leading to recurrence and  
207 progression. Post-operative chemotherapy and radiotherapy have considerable cumulative side effects (17–19),  
208 including impaired cognitive function (14). Studies have also shown very limited benefit for HGG patients  
209 undergoing re-resection of residual tumour (20), and highlight the psychosocial impact of a brain tumour  
210 diagnosis for TYA patients (14). As efforts to improve survival continue, it remains imperative to minimise  
211 short- and long-term side-effect profiles or find more targeted alternatives better suited to these complex  
212 tumours.

213 In this study, we have investigated a series of TYA HGGs integrating DNA methylation, mutational analysis,  
214 neuropathological and clinical annotations, and identified novel tumour subgroups with distinctive methylation  
215 profiles.

216

217

218

219

220

221

222

223

224

225

226

227

228

229  
230  
231  
232  
233  
234  
235  
236  
237  
238  
239  
240  
241  
242  
243  
244  
245  
246  
247  
248  
249  
250  
251  
252  
253  
254  
255  
256  
257  
258  
259  
260  
261  
262  
263  
264

## **Materials and Methods**

### **Cases**

A total of 398 samples were collected from national and international collaborators (tumour samples: University College London Hospitals, London, n = 63; internal biobank, n = 58; King's College Hospital, London, n = 39; Southampton General Hospital, n = 38; The Chinese University of Hong Kong, n = 37; Salford NHS Foundation Trust, n = 33; Royal Preston Hospital n = 29; Bambino Gesù Children's Hospital, Rome, n = 26; Queensland Children's Tumor Bank, Brisbane, n = 23; University Hospitals Bristol, n = 17; Great Ormond Street Hospital, London, n = 15; Poland, n = 11; Children's Cancer Institute and Sydney Children's Hospital, n = 9). Where possible, both formalin-fixed paraffin-embedded (FFPE) and/or frozen tissue was provided for each case. Data were also retrieved and integrated from previously published studies from the Jones Lab (2,16,21). Patients were selected according to age ( $\geq 13$  -  $\leq 30$  years old) and diagnosis (IDH/H3-wildtype glioma, WHO grade 2, 3 or 4). Definitions of TYA age are variable, with the UK stating that the age range is between 16 – 24 years (22); for this study, we decided to broaden the age to  $\geq 13$  -  $\leq 30$  years old to ensure the age distribution for each tumour subtype could be captured. Cases were excluded if they were diagnosed at the centre of origin/classified as a well-characterised subtype of high-grade glioma according to the WHO 2021 (astrocytoma, IDH-mutant; diffuse midline glioma, H3 K27-altered; diffuse hemispheric glioma H3 G34-mutant). All CNS WHO grade 1 gliomas and glioneuronal tumour diagnoses were excluded, alongside non-gliomas (ependymal, embryonal, mesenchymal, and germ cell tumours). Tissue samples obtained from the University Hospital Southampton NHS Foundation Trust, Royal Preston Hospital, Great Ormond Street Institute for Child Health, University College London Hospitals, Southmead Hospital, and the Northern Care Alliance as part of BRAIN UK, were supported by Brain Tumour Research, the British Neuropathological Society and the Medical Research Council.

A final cohort of 207 samples was investigated.

### **Consent and ethics statement**

Written informed consent was obtained for all samples included in this study, under Research Ethics Committee approval at each participating centre. Project specific Research Ethical Approval was also received via application to BRAIN UK (23).

265 **Nucleic Acid Extraction**

266

267 DNA and RNA were extracted from frozen tissue using the *Quick-DNA/RNA* Miniprep Plus Kit (Zymo)  
268 according to manufacturer's instructions. For FFPE tissue, DNA was extracted where possible after manual  
269 macro-dissection using the QIAamp DNA FFPE Tissue Kit protocol (QIAGEN) and RNA was extracted using  
270 the AllPrep DNA/RNA kit (Qiagen) according to manufacturer's instructions.

271

272 **Methylation Profiling**

273

274 Analysis was performed using Illumina EPIC BeadArrays at University College London (UCL) Great Ormond  
275 Street Institute of Child Health when more than 140 ng of DNA was extracted. Data from EPIC arrays was pre-  
276 processed using the minifi package in R (v1.48.0). 15 Italian cases were analysed at Bambino Gesù Children's  
277 Hospital and raw data were shared and included for the bioinformatic analyses. Data from EPIC arrays was pre-  
278 processed using the minifi package in R (v1.48.0). A cohort of 207 cases met the entry criteria and could  
279 progress into the study. The Heidelberg brain tumour classifier (moleculareuropathology.org) was used to  
280 assign a calibrated score to each case, associating it with one of the >100 tumour entities which feature within  
281 the classifier (v12.8). Tumours were subclassified into one of 17 methylation subgroups; diffuse paediatric-type  
282 high grade glioma, H3 wildtype and IDH wild type, Subtype A/B (pedHGG\_A/B), diffuse paediatric-type high  
283 grade glioma, MYCN subtype (pedHGG\_MYCN), diffuse paediatric-type high grade glioma, RTK1 subtype,  
284 subclass A/B/C (pedHGG\_RTK1A/B/C), diffuse paediatric-type high grade glioma, RTK2 subtype, subclass  
285 A/B (pedHGG\_RTK2A/B), glioblastoma, IDH-wildtype, subtype posterior fossa (GBM\_CBM), adult-type  
286 diffuse high grade glioma, IDH-wildtype, subtype E (HGG\_E), adult-type diffuse high grade glioma, IDH-  
287 wildtype, subtype B (HGG\_B), glioblastoma, IDH-wildtype, RTK1 subtype (GBM\_RTK1), glioblastoma, IDH-  
288 wildtype, RTK2 subtype (GBM\_RTK2), glioblastoma, IDH-wildtype, mesenchymal subtype, typical/atypical  
289 (GBM\_MES\_TYP/ATYP), pleomorphic xanthoastrocytoma (PXA), and high-grade astrocytoma with piloid  
290 features (HGAP). Clustering of beta values from methylation arrays was performed based upon correlation  
291 distance using a ward algorithm. Quality control was undertaken; the methylation data for samples where the  
292 probe failure rate was >20% or bisulphite conversion failed were excluded from the methylation analysis.  
293 However, they were not excluded from the study and were analysed with other workflow streams. Mean p-value  
294 detection is a common QC filtering criteria and is advised by Illumina. However, the probe failure rate is not  
295 stringent because of the inclusion of historical FFPE cases. To date, Illumina do not provide specific guidelines  
296 on the cut-off and advise discretion. The MNP classifier uses 10,000 probes; cases with a probe failure rate  
297  $\leq 20\%$  showed concordance with MNP assignments, t-SNE location, and clinical/genomic case annotations.

298

299 Samples were assigned a methylation subgroup when the calibrated score was >0.5, and after correlating with  
300 the histological diagnosis and available molecular data. Samples with a calibrated score of <0.5, or if the  
301 assignment was not appropriate, were assigned as NEC (not elsewhere classified), as per the WHO classification  
302 definition, and underwent further characterisation to determine their subtype.

303

304 **Reference cohorts**

305  
306  
307  
308  
309  
310  
311  
312  
313  
314  
315  
316  
317  
318  
319  
320  
321  
322  
323  
324  
325  
326  
327  
328  
329  
330  
331  
332  
333  
334  
335  
336  
337  
338  
339  
340  
341  
342  
343  
344

Classifier results for the TYA cohort were plotted against a t-SNE reference cohort of CNS tumours, composed of 8488 pairs of publicly available methylation iDats for different brain tumour types that are part of the classifier (derived from accession numbers E-MTAB-3476, E-MTAB-4969, E-MTAB-5797, E-MTAB-7490, E-MTAB-8390, E-MTAB-8888, GSE103659, GSE104210, GSE104293, GSE109330, GSE109381, GSE116298, GSE117130, GSE119774, GSE122038, GSE122920, GSE122994, GSE123678, GSE124617, GSE125450, GSE128654, GSE131482, GSE133801, GSE135017, GSE136361, GSE137845, GSE138221, GSE140124, GSE143843, GSE147391, GSE152653, GSE156012, GSE156090, GSE157397, GSE164994, GSE166569, GSE183656, GSE183972, GSE184900, GSE188547, GSE190362, GSE193196, GSE196490, GSE197378, GSE198855, GSE200647, GSE215240, GSE36278, GSE52556, GSE55712, GSE60274, GSE61160, GSE65362, GSE70460, GSE73801, GSE73895, GSE85218, GSE92577, GSE92579), TCGA\_GBM and TCGA\_LGG. Entry into the reference cohort was determined by the same quality control metrics as for the TYA cohort. Data was derived from 450K and 850K array data and was combined using combineArrays() functionality from minfi, reducing both arrays to their common set of probes. The reference cohort therefore comprised methylation profiles for the spectrum of different brain tumour types, irrespective of age, that the TYA methylation cohort could be compared with in terms of their t-SNE cluster locations, and allowed the exclusion of any cases that classified or aligned with non-glioma tumours. Gender information was available for 4653 cases, 2109 cases were from female patients, and 2544 from male patients. Age was available for 5078 cases (median 19 years, range 0.1-93 years). The glioma reference cohort was derived by filtering the CNS reference cohort for the different glial subtypes (specifically high-grade glial tumours). Cohorts of all the existing HGG entities that are currently part of the v12.8 classifier were represented. Gender information was available for 1446 cases (604 female, 842, male). Age was available for 1434 cases (median 25 years, range 0.1-86 years). These were plotted in a separate t-SNE, and the TYA cohort was then plotted with them, to observe more clearly the clustering of the different HGG subgroups in the TYA population.

### **DNA copy number**

DNA copy number was recovered from combined intensities using the conumee package (v1.36.0). This was derived from combined  $\log_2$  intensity data based upon an internal median processed using the R packages minifi and conumee to call copy number in 15,431 bins across the genome. Samples were arranged in columns clustered by contiguous categorical copy number states based upon log ratio thresholds of  $\pm 0.1$  for gain/loss and  $\pm 0.5$  for amplification and deletion, and organised by their DNA methylation subgroups. Clustering used Euclidean distance and a ward algorithm.

### **Fusion Panel**

RNA was successfully extracted from 128 samples. Library preparation was completed using FUSIONPlex™ Pan Solid Tumor v2 panel (Archer) following manufacturer's instructions. Libraries were pooled and sequenced aiming to target 2.5M reads per sample. Analysis was performed using Archer® Analysis Unlimited (software v7.1).

345  
346  
347  
348  
349  
350  
351  
352  
353  
354  
355  
356  
357  
358  
359  
360  
361  
362  
363  
364  
365  
366  
367  
368  
369  
370  
371  
372  
373  
374  
375  
376  
377  
378  
379  
380  
381  
382  
383  
384

## **DNA Sequencing**

Whole exome sequencing was performed for 107 cases using Agilent SureSelect whole exome v8 at the Institute of Cancer Research core genomics facility. Libraries were pooled and sequenced appropriately aiming for 300x depth. Matched germline DNA was available for 27 samples, which were prepared as above and sequenced at 100x depth. Exome capture reads were aligned to the hg19 build of the human genome using bwa v0.7.12 (bio-bwa.sourceforge.net), and PCR duplicates removed with PicardTools 1.94 (pcard.sourceforge.net). Single-nucleotide variants were called using the Genome Analysis Tool Kit v3.4–46 based upon current best practices using local realignment around indels, down sampling, and base recalibration with variants called by the Unified Genotyper (broadinstitute.org/gatk/). Variants were annotated using the Ensembl Variant Effect Predictor v74 (ensembl.org/info/docs/variation/vep) incorporating SIFT (sift.jcvi.org) and PolyPhen (genetics.bwh.harvard.edu/pph2) predictions, COSMIC v64 (sanger.ac.uk/genetics/CGP/cosmic/), dbSNP build 137 (ncbi.nlm.nih.gov/sites/SNP), ExAc, and ANNOVAR annotations.

## **Neuropathology assessment**

The original slides were centrally reviewed, blinded to the molecular profile. Tumours were reviewed with reference to microscopic criteria reported in the WHO Classification of Tumours of the Central Nervous System, 5<sup>th</sup> Edition 2021 including the degree of cellularity, atypia, presence of mitoses, microvascular proliferation and necrosis (10). Differences in cytological or architectural appearances were noted and subsequently reviewed in the context of molecular profile.

## **Statistical Analysis**

Statistical analysis was carried out using R 4.3.2 (www.r-project.org) and GraphPad Prism 9. Categorical comparisons of counts were carried out using Fisher exact test; comparisons between groups of continuous variables employed Student t test or ANOVA. Univariate and multivariate differences in survival were analysed by cox regression to determine the hazard ratios and significance. All tests were two-sided and a P value of less than 0.05 was considered significant after multiple testing correction (FDR).

## **Data Availability**

All newly generated data have been deposited in the European Genome–phenome Archive (www.ebi.ac.uk/ega) with accession number EGAS50000000641 (sequencing) or ArrayExpress (www.ebi.ac.uk/arrayexpress/) with accession numbers E-MTAB-13974 and E-MTAB-13975 (methylation arrays). Curated gene-level copy number and mutation data are provided as part of the paediatric-specific implementation of the cBioPortal genomic data visualisation portal (pedcbioportal.org). The summary data can also be accessed via Synapse (accession number 64620613). Raw data from this study are available upon request to the corresponding author.

385  
386  
387  
388  
389  
390  
391  
392  
393  
394  
395  
396  
397  
398  
399  
400  
401  
402  
403  
404  
405  
406  
407  
408  
409  
410  
411  
412  
413  
414  
415  
416  
417  
418  
419  
420  
421  
422  
423

## Results

### The TYA HGG cohort

Two-hundred and seven of the collected samples, from patients aged 13-30 years at diagnosis and from any location within the CNS, underwent DNA methylation profiling, of which 107 cases also underwent whole exome sequencing, and were confirmed to be *IDH*- and histone-wildtype high-grade glioma (**figure 1A**). Tumour location was available for 189 cases; 84.7% (n=160) were hemispheric, and 15.3% (n=29) were identified in a midline anatomical location (**figure 1B**). 44.4% (n=92) of the collected cohort were female, and 55.6% (n=115) were male (**supplementary figure 1A**). The median age was 17.0 years (range 13–30 years). Where the histological diagnosis was available, 83.7% (n=154/184) were diagnosed histologically as a glioblastoma or high-grade glioma; rare cases formerly known as PNET and anaplastic pleomorphic xanthoastrocytoma (PXA) were included due to no available molecular confirmation of these diagnoses. Review of the histology (where available) showed high cellularity, microvascular proliferation, necrosis, and increased mitotic activity. 7.6% (n=14) were diagnosed as a form of anaplastic glioma (a term no-longer recognised by the WHO classification in the context of glioma subtypes) (**supplementary figure 1B**).

Outputs from DNA methylation profiling was used to filter cases with poor quality control (QC), and those classified as ‘NOS’ due to calibrated scores lower than 0.5. A pan-CNS reference cohort, consisting of 8488 cases from existing publicly available datasets (2,8,16,21,24,25), was constructed and plotted using t-SNE projections (**supplementary figure 2A**).

Twelve cases did not meet the methylation data QC requirements and so were not included in the methylation data analysis, but remained in the cohort and were processed as per other elements of the study. Thirty-seven cases were assigned ‘NOS’, requiring further characterisation using alternative integrated diagnostic approaches (**figure 1C**). The NOS group did not form distinct methylation clusters using t-SNE, suggesting they did not represent a novel subgroup(s). The remaining 158 cases (excluding NOS cases) were projected onto a reference set of gliomas comprising several HGG entities (n=3357) (**figure 2A, (supplementary table 1)**). Twenty-nine cases (18.0%) were classified as subgroups more frequently seen in older adults (by current classifier definitions) including GBM\_MES (n=25, 15.5%), GBM\_RTK1/2 (n=4, 2.5%). 15.5% (n=25) cases classified as

424 a pleomorphic xanthoastrocytoma (PXA) and 5.0% (n=8) as high-grade astrocytoma with piloid features  
425 (HGAP), a new entity in the WHO classification.

426  
427 Clinical treatment information was available for nine cases classifying as PXA. 7/9 PXA cases achieved a GTR,  
428 a single tumour was debulked and one received a biopsy only. All 9 cases were treated with chemotherapy  
429 (reported to be temozolomide in 5 cases) and radiotherapy, and two cases were treated with radiotherapy alone.  
430 Two cases were treated with trametinib and dabrafenib. A combination of dabrafenib and vemurafenib was used  
431 for two cases diagnosed as 'anaplastic PXA'. Survival data comparing PXA with HGAP showed a similar  
432 overall survival profile (median OS 28 months vs 34 months respectively,  $p=0.5393$  ns) (**supplementary figure**  
433 **2B**).

434  
435 Overall, this demonstrated that a relatively small proportion of TYA *IDH*- and H3-wildtype HGGs represent  
436 tumour types associated with the adult population.

### 437 438 **Paediatric-specific and novel methylation subgroups**

439  
440 When reviewing the classifier assignments and tSNE distribution of the 158 cases (excluding NOS cases),  
441 eighty-six (54.4%) classified as paediatric-type subgroups (by current classifier definitions) including pedHGG-  
442 RTK1A/B/C (n=51, 32.3% (47.1% n=24 RTK1A, 31.4% n=16 RTK1B, 21.6% n=11 RTK1C), pedHGG-*MYCN*  
443 (n=13, 8.2%), and pedHGG-RTK2A/B (n=12, 7.6% (75.0% n=9 pedHGG-RTK2A, 25.0% n=3  
444 pedHGG-RTK2B). Twenty-three cases were assigned to novel, recently identified, poorly-characterised  
445 subgroups with distinct methylation profiles including adult-type diffuse HGG, *IDH*-wildtype, subtype B  
446 (HGG\_B, n=2, 1.3%), adult-type diffuse HGG, *IDH*-wildtype, subtype E (HGG\_E, n=6, 3.8%), glioblastoma,  
447 *IDH*-wildtype, subtype posterior fossa (GBM-CBM, n=5, 3.2%) and pedHGG-A/B (n=10, 6.3%) (**figure 2A**).

448  
449 The 158 cases were then plotted in a t-SNE alone (**figure 2B**). They maintained the expected pattern of  
450 clustering according to their methylation profiles, including clustering of those subgroups associated with  
451 paediatric populations (e.g., pedHGG\_A/B/RTK/*MYCN* etc.) and adult population (GBM\_MES\_TYP/ATYP).  
452 Similar patterns of clustering to that seen in the glioma reference t-SNE was observed, helping to validate the  
453 assignments. This was also confirmed using unsupervised clustering; the pedHGG-RTK tumours clustered  
454 together as did the MAPK-pathway driven tumours (PXA and HGAP cases). Interestingly, the HGG\_E cohort  
455 formed a distinct cluster with a hypo-methylated profile (**supplementary figure 2C**).

456  
457 The majority of TYA HGG *IDH*- and H3-wildtype HGGs therefore classify as either a paediatric-type or a  
458 poorly understood novel methylation class.

### 459 460 **Incidence of tumour subtypes in the TYA age group**

461

462 To explore the relationship between age and frequency across the different HGG groups and subgroups, we  
463 investigated publicly available methylation datasets in combination with our data (n=8488) to create age-density  
464 plots for each methylation-defined subgroup of HGG (**figure 2C**).

465  
466 PedHGG\_RTK1B (n=37, median age 16.6 years, age-density peak 13.1 years), and pedHGG\_B (n=23, median  
467 age 31.4 years, age-density peak 16.2 years) show a large proportion of their frequency (n=27/38 and n=11/23  
468 respectively) within the TYA age spectrum of 13-30 years. pedHGG\_RTK1A (n=124, median 16.6 years, age-  
469 density peak 13.1 years) and pedHGG\_RTK1C (n=53, median 22.4 years, age-density peak 13.9 years) also  
470 frequently occurred within the TYA age group (n=54/124 and n=24/53 respectively). Of those cases classifying  
471 as pedHGG\_RTK1, seven cases underwent GTR, three debulking procedures, two subtotal resections and a  
472 single case of biopsy only. Fifteen cases were treated with adjuvant chemotherapy (most frequently  
473 temozolomide) and fourteen treated with combined radiotherapy. Two patients were treated with chemotherapy  
474 or radiotherapy alone. Single cases were treated with a peptide vaccine, bevacizumab, and palliative  
475 immunotherapy (nivolumab).

476  
477 Glioblastoma, RTK1 (n=213, median age 59.4 years, age-density peak 61.4 years), RTK2 (n=350, median age  
478 58.4 years, age density peak 54.2 years), and MES\_TYP (n=311, median age 54.5 years, age-density peak 61.6  
479 years) subtypes show an age distribution of patients aged >50 years. GBM\_MES\_ATYP (n=40, median age  
480 32.7 years, age-density peak 15.0 years), distinct from the GBM\_MES\_TYP group, show that 38% (n=15/40) of  
481 cases fall within the TYA age group. The pedHGG\_RTK1 subgroups also showed a similar distribution, with a  
482 higher incidence in the TYA age group compared to the paediatric age group (n=105/215 vs n=86/215  
483 pedHGG\_RTK1), but they are not exclusive to this age. No subgroups show all of their distribution within the  
484 TYA age group. With consideration to the number of cases in each subgroup cohort, many of the curves showed  
485 a tail characterised by smaller peaks of density occurring outside their peak distribution, and in some subgroups  
486 their expected range (e.g., paediatric-type tumours occurring in older adults and adult-specific tumours  
487 occurring in the paediatric setting). pedHGG\_RTK2A tumours (n=58, median age 13.3 years, age-density peak  
488 12.7 years) showed a greater proportion of cases in the TYA age group than the pedHGG\_RTK2B tumours  
489 (n=41, median age 19.7 years, age-density peak 9.1 years) with n=25/58 and n=9/41 respectively. Clinical  
490 annotations for cases classifying as pedHGG\_RTK2, indicated one case had a subtotal resection and two  
491 underwent biopsy only. Three were treated with both chemotherapy and radiotherapy, one of which was  
492 craniospinal due to the identification of metastatic spinal lesions. Chemotherapy consisted of adjuvant  
493 temozolomide and second line procarbazine and lomustine. Re-irradiation was reported in a single case.  
494 Survival data for the paediatric-type HGG subgroups showed similar survival profiles (median OS for  
495 pedHGG\_MYCN 13.0 months, pedHGG\_RTK1C 23.0 months, pedHGG\_RTK2A 14.7 months, pedHGG\_A  
496 14.0 months, pedHGG\_B 20.1 months) (**supplementary figure 2D**).

497  
498 For the poorly characterised methylation subgroups, HGG\_E cases show a broad range of incidence with a peak  
499 at approximately 9.4 years but a median age of 15.8 years (n=23, range 2 - 64 years), with cases identified  
500 across both the paediatric, adolescent and young adult ages but declining to very low incidences after age 30  
501 (**figure 2C**). HGG\_B cases (n=8, median age 35.1 years, age density peak 29.1 years) showed a higher

502 frequency of cases in the TYA age group, though numbers are small (n=6/7). According to the current classifier  
503 definition of the HGG\_B and HGG\_E groups, they were both ‘adult-type’ diffuse HGG but such a definition  
504 was not reflected by either of the density profiles. The GBM\_CBM group (n=26, median age 26.8 years)  
505 showed n=13/26 cases occurring in the TYA age group, with a peak at 15.6 years and a range of 2 – 74 years.  
506 The pedHGG\_B subgroup mimics the trend seen with the GBM\_CBM group. The pedHGG\_A group (n=25)  
507 has a median age of 13.8 years, and the incidence then declines after age 30 years, with a range of 1.3 to 57  
508 years. Clinical annotations for novel entities showed that three cases achieved GTR, and single incidences of  
509 STR, tumour debulking and biopsy alone. One case of GBM\_CBM was treated with adjuvant radiotherapy in  
510 addition to bevacizumab and is alive at the time of writing. 4/5 HGG\_E cases were treated with adjuvant  
511 chemotherapy (temozolomide) and radiotherapy, with the remaining case treated with chemotherapy alone.

512  
513 When comparing to other molecularly-defined HGG subtypes, the infant-type hemispheric gliomas (IHG)  
514 (n=66, median age 2.3, age-density peak 0.5 years) characteristically occur in the infant population, the diffuse  
515 hemispheric glioma, G34-mutant (DHG\_G34) (n=181, median age 19.1 years, age-peak 14.3 years) and IDH-  
516 mutant high-grade astrocytomas (A\_IDH\_HG) (n=221, median age 35.6 years, age-density peak 32.9 years),  
517 and diffuse midline glioma, H3 K27-altered (DMG\_K27) (n=357, median age 11.4 years, age-density peak 6.5  
518 years) show a proportion of their frequency within the TYA age spectrum of 13-30 years (**supplementary**  
519 **figure 2E**).

520  
521 Therefore, no methylation subclasses of HGG are exclusive to the TYA age group, although some show a peak  
522 in their distribution in the 13-30 year range (including HGG\_B, GBM\_CBM and GBM\_MES\_ATYP), and  
523 more generally, paediatric- and adult-type HGG groups show a wider age distribution than perhaps would be  
524 expected.

### 525 526 **Copy number profiling**

527  
528 Copy number data derived from the Illumina array, was available for all 207 cases. Review of the clinical  
529 annotations associated with the glioma reference cohort identified that 8310/11933 (69.6%) cases were  
530 annotated for age, and of these 276 cases correlated with the study inclusion criteria and were within the TYA  
531 age range. After excluding cases classified as NOS or failing to meet the methylation QC parameters, 158 cases  
532 were combined with those derived from the glioma reference cohort (giving a total of n=434) and were clustered  
533 within their respective methylation subgroups (**figure 3A**). Subtype-enriched profiles were observed, including  
534 the classical gain of chr7 and loss of chr10 seen in the GBM\_MES\_TYP and GBM\_RTK1 subgroups,  
535 consistent with the pattern of adult HGG. The methylation-defined paediatric-specific subgroups showed more  
536 variable profiles with changes frequently involving chr1. The pedHGG\_MYCN tumours were enriched for gains  
537 of chr1, 2 and 7.

538  
539 When the same cohort was clustered by copy number change across the methylation subgroups, frequent  
540 changes across the cohort included chromosomal gains (chr1q (54%), chr2 (22%), chr7 (41%)) and losses  
541 (chr10 (40%), chr13 (64%)) (**supplementary figure 3**).

542  
543  
544  
545  
546  
547  
548  
549  
550  
551  
552  
553  
554  
555  
556  
557  
558  
559  
560  
561  
562  
563  
564  
565  
566  
567  
568  
569  
570  
571  
572  
573  
574  
575  
576  
577  
578  
579  
580

Focal amplifications seen in the cohort included *PDGFRA* (5.8%), *CDK4* (3.9%), *MYCN/ID2* (4.3%), *MYC* (1.4%), *CDK6* (1.4%) and *EGFR* (1.0%) and the most common focal deletion was *CDKN2A/p16* (19.2%). Across the combined cohort of 434 cases, similar patterns were seen, but also amplifications in *KIT* (n=14, most frequent in pedHGG\_RTK1B subgroup), *MET* amplifications (n=4, seen in pedHGG\_RTK1C (n=2), HGG\_B (n=1) and PXA (n=1) subgroups) and a higher frequency of *EGFR* amplifications (n=15, seen across GBM\_RTK2 (n=4), pedHGG\_MYCN (n=4), pedHGG\_RTK2A (n=4) and pedHGG\_A (n=3) subgroups) were identified (**figure 3B, 3C, supplementary tables 2 & 3**).

TYA HGG therefore show the characteristic copy number changes, and gene amplifications and deletions, which are known to occur across the HGG spectrum, but are enriched in specific methylation subclasses.

### **Somatic mutational landscape of TYA HGG subgroups**

Whole exome sequencing data was available in 107/207 cases (**figure 4, supplementary table 4**). Twenty-seven cases assigned as NOS (calibrated score <0.5) and 12 cases whose methylation data were excluded due to inadequate QC parameters also underwent WES. Cases were grouped according to their HGG subgroup based on their DNA methylation profiles; some of the variants detected (and the pattern of incidence) from the NOS and methylation QC-failed group paralleled the known methylation profiles. The essential and desirable diagnostic criteria from the current WHO classification (12) were applied when grouping these cases accordingly. If the methylation or variant profiles could not support a reliable assignment, they were grouped according to the variant type seen e.g., MAPK pathway-altered (n=8), *MYCN*-amplified (n=2), and *CDKN2A/B/p16*-deleted (n=6).

Pathognomonic mutations of tumour subgroups were detected, including the presence of *CDKN2A/B* alterations and MAPK pathway alterations (e.g., *BRAF* V600E mutations) in PXA (n=9), and *CDKN2A/B* alterations and *ATRX* mutations in HGAP (n=3). The most frequent glioma-associated variants included *TP53* (n=65), *NF1* (n=35), *PDGFRA* (n=28), and *EGFR* (n=18) (**supplementary figure 4A**).

Eight cases from the cohort showed a hypermutator phenotype (mutation frequency ranging from 2817-5273) with frequent mutations in *TP53*, *ATRX*, *PDGFRA*, *BCOR*, *SED2*, *NF1*, and *RBI* (**figure 4**). Three of these cases classified as the novel HGG\_E methylation subgroup, suggesting a somatic mutational signature of this group. Others included pedHGG\_RTK1 (n=1) and GBM\_CBM (n=1) cases, and also tumours which did not classify as any of the currently recognised entities n=3, NOS).

Current adult defined subtypes including GBM\_MES (n=15) and GBM\_RTK1 (n=3) were enriched for the presence of *PTEN* variants (n=8/18) and *CDK4* amplifications (n=2/3 in GBM\_RTK1), in addition to frequent variants in *TP53* (n=12/18).

581 The current paediatric subtypes also showed distinct signatures compared to other subgroups of HGG; as  
582 expected, the pedHGG\_RTK1A/B/C subgroups were all enriched for *PDGFRA* alterations (mostly  
583 amplifications) (n=11/16) as well as *TP53* (n=11/16) and *ATRX* (n=6/16) variants, and variable incidences of  
584 *CDKN2A/B*, *BCOR*, *SETD2* and *NF1* alterations (**figure 4**). Nine cases were assigned to a ‘pedRTK1-like’  
585 group based on *PDGFRA* (n=8) alteration. The pedHGG\_*MYCN* was associated with *MYCN* amplifications,  
586 although this was not a universal feature of high-scoring tumours in the *MYCN* subgroup (n=3/7). 2 further  
587 NOS/methylation QC-failed cases contained a *MYCN* amplification and in the absence of other subgroup-  
588 identifiable features, were assigned to a *MYCN*-like group.

589

590 Three cases classifying as the novel GBM\_CBM group showed a variable incidence of variants including  
591 hypermutator phenotype in one case, *ATRX* and *PDGFRA* variants, and non-specific range of variants in genes  
592 frequently mutated in HGG including *BCOR*, *SETD2*, *NF1*, *RBI* and *CDK4* amplifications.

593

594 Eight cases contained variants frequently seen in HGG, but the profile of these and the available  
595 neuropathological or molecular data did not support a reliable assignment and they were therefore grouped as  
596 ‘HGG\_Other’ (**figure 4**).

597

598 ArcherDX fusion panel sequencing was performed on 92/207 (44.4%) cases (**supplementary figure 4B**), and  
599 identified isolated examples of RTK fusions (*PRPTZ1::MET* and *GOPC::ROS1* fusions). These alterations were  
600 validated by indicative small copy number changes, showing that RTK fusions are not a frequent feature in  
601 TYA HGG. A single *KIAA1549::BRAF* fusion was identified in an HGAP case, which is a recognised molecular  
602 feature in a subset of these tumours.

603

604 TYA HGG therefore show mutational landscapes which may be targetable, and an integrated diagnostic  
605 approach can be used to assign cases to methylation- or variant-based cohorts to help guide management.

606

### 607 **Characteristics of poorly-described methylation-defined subgroups and clinical correlations**

608

609 This study has identified three HGG subgroups occurring more frequently in the TYAs including GBM\_CBM,  
610 HGG\_B and GBM\_MES\_ATYP, all of which were considered poorly-described methylation subgroups. We  
611 gathered all publicly available data, and from a local adult-based diagnostic centre, for these rare groups,  
612 irrespective of age, to review their characteristic features (HGG\_B (n=19), GBM\_CBM (n=34) and  
613 GBM\_MES\_ATYP (n=102)). The GBM\_MES\_ATYP subgroup occurred more frequently in males (n=62/102)  
614 (**figure 5A**). The median age for GBM\_CBM was 36.8 (range 9–77 years), GBM\_MES\_ATYP was 50.4 (range  
615 1–82 years) and HGG\_B was 29 (range 23–78 years) (**figure 5B**). There is a peak of distribution in the TYA age  
616 group for GBM\_CBM and GBM\_MES\_ATYP. However, for the GBM\_CBM subgroup, there is a long tail of  
617 distribution extending into older adults, and for the GBM\_MES\_ATYP, a large, broad peak in older patients.  
618 The HGG\_B subgroup however, is a TYA-specific subgroup. Although the current naming of the GBM\_CBM  
619 group implies they occur in the cerebellum, this is not always the case with 4/27 cases (14.8%) with available

620 location information reported in a hemispheric location (either frontal or temporal lobes), and single cases in the  
621 thalamus and spinal cord (**figure 5C**).

622

623 Histology showed features consistent with a HGG including the presence of multinucleated giant cells for all  
624 subtypes (**Figure 5D, supplementary figure 5A**). The TYA-specific HGG\_B subgroup showed heterogenous  
625 appearances. Some tumours showed perinuclear clearing (**figure 5D1-4**) with round to oval atypical nuclei.  
626 However, they also showed variable architectural features; rare cases showed a nested architecture surrounded  
627 by a more fibrous-like stroma (**figure 5D4**) and others showed a low to moderate cellularity with a more  
628 infiltrative pattern (**figure 5D5**). A single case showed focal areas with an embryonal-like appearance  
629 comprising hyperchromatic and pleomorphic irregular shaped nuclei which showed a distinct palisading  
630 architectural pattern (**figure 5D6**). 3/9 cases showed the presence of microcalcifications. GBM\_CBM histology  
631 showed a highly cellular and infiltrative glial tumour, with a subset of cases showing perinuclear clearing, set  
632 within a fibrillary stroma (**supplementary figure 5A1-5**). The nuclei were round to oval, with variable degrees  
633 of nuclear pleomorphism (**supplementary figure 5A5**). Some cases showed oval-shaped or spindle nuclei, and  
634 others contained cells with a ‘pennies on a plate’ or multinucleated morphology (**supplementary figure 5A1-5**).  
635 Small, thin-walled branching vessels were interspersed within the tumours. GBM\_MES\_ATYP cases comprised  
636 a highly cellular glial tumour set within a fibrillary stroma. The tumour cells formed a dense sheet-like  
637 architecture. The nuclei showed variable degrees of atypia (including very markedly atypical and large nuclei),  
638 and frequently displayed pale chromatin with prominent nucleoli, surrounded by pink eosinophilic pale, granular  
639 or glassy cytoplasm (**supplementary figure 5A6-10**). Multinucleated cells were also common (**supplementary**  
640 **figure 5A6-8**). Rare cases showed focal collections of more primitive appearing cells (**supplementary figure**  
641 **5A9**), and frequently cases showed distinct areas of inflammatory cell infiltrates (12/39 cases) (**supplementary**  
642 **figure 5A10**). Limited available survival data shows that the HGG\_B, GBM\_CBM and GBM\_MES\_ATYP  
643 groups have a poor prognosis (median OS 19.1, 22.6 and 7 months respectively) (**figure 5E**).

644

645 Copy number profiling data for HGG\_B (n=19) showed considerable variability with no distinctive patterns  
646 (**figure 5F**). GBM\_CBM (n=34) also showed considerable variability with no distinctive differences between  
647 patients aged <30 or >30 years (**supplementary figure 5B**). The GBM\_MES\_ATYP cases (n=102) showed  
648 frequent gains of chr7 associated with chr10 loss (18.6%, n=19/102) compared to GBM\_MES\_TYP (15.2%,  
649 n=5/33, p=0.7960), but also a proportion of cases which contained just chr7 gains (19.6%, n=20/102), lower  
650 than the proportion with this change seen in GBM\_MES\_TYP (27.3%, n=9/33, p=0.3421). When looking at  
651 cases of GBM\_MES\_ATYP aged <30, these cases were more frequently associated with a gain of chr7 alone  
652 (36.8% n=7/19) compared to those aged >30 (15.6%, n=13/83, p=0.0528), and a subset of these were also  
653 associated with a gain of chr1 (21.1%, n=4/19), and a proportion of cases containing gains of chr6 (21.1%,  
654 4/19). There was a higher frequency of cases which contained neither change in the GBM\_MES\_ATYP group  
655 (40.2%, n=41/102) compared to GBM\_MES\_TYP (30.3%, n=10/33, p=0.4092) (**supplementary figure 5B**).  
656 Sequencing data shows *TP53* variants (n=5/6) and amplifications including *MYCN* (n=1/6), *EGFR* (2/6), *MET*  
657 (1/6), *CDK4* (1/6) and *PDGFRA* (1/6) in the HGG\_B cases (**figure 5G**). There is enrichment of *CDKN2A/B*  
658 deletions in the GBM\_CBM group (n=7/10), and *RBI* (n=3/13), *PTEN* (n=6/13), *NF1* (n=5/13) and *TP53*  
659 (10/13) alterations occurring more frequently in the GBM\_MES\_ATYP group (**supplementary figure 5C**).

660 When plotting methylation data of GBM\_MES\_ATYP cases alone into a tSNE and annotating them by age, no  
661 age-defined clustering was seen (**supplementary figure 5D**).

662

663 Clinically, 3/5 GBM\_MES cases achieved a GTR with two cases of subtotal resection. Three cases reported  
664 treatment with adjuvant chemotherapy and radiotherapy. In addition, one patient received nivolumab,  
665 ipilimumab, and regorafenib during the course of their treatment. Re-irradiation was used in a single case. Cases  
666 classifying as GBM\_MES\_TYP showed an improved survival when compared to the GBM\_MES\_ATYP group  
667 (median OS 18 months vs 7 months,  $p=0.05463$ ) (**supplementary figure 5E**).

668

669 Several cases associated with tumour predisposition syndromes were identified; interestingly, two patients were  
670 siblings (Glio\_0021, Glio\_0029). Glio\_0021 was reported to have Turcot's/mismatch repair syndrome and  
671 Glio\_0029 was reported to have constitutional mismatch repair deficiency syndrome (CMMRD). Both tumours  
672 showed histological features of a high-grade glioma, with the presence of multinucleated cells (**figure 6A**), and  
673 were hypermutant, but classified differently by methylation profiling (pedHGG\_RTK1A and HGG\_E  
674 respectively) (**figure 6B,C,D**). Glio\_0004 was identified to have Li Fraumeni syndrome, and Glio\_0272 (HGG  
675 classifying as a pedHGG\_RTK1A) was found to have bi-allelic somatic inactivation of *MSH2*, but germline  
676 samples were not available.

677

678 6/70 cases (8.6%) were treated for a previous childhood malignancy before the diagnosis of an HGG (**figure**  
679 **6E**); Glio\_0228 was treated for a tectal plate pilocytic astrocytoma (including radiotherapy), but was  
680 subsequently diagnosed with an HGG eleven years later, in a similar location, classifying as an HGG\_E tumour.  
681 Glio\_0219 had a history of acute lymphoblastic leukaemia (ALL) as a child, treated with chemotherapy and  
682 whole body radiotherapy, and was subsequently diagnosed with an HGG aged 22 which classified as  
683 pedHGG\_RTK1B. Similarly, Glio\_0226 was also treated for ALL as a child with chemotherapy, and then  
684 diagnosed with a pedHGG\_RTK1B tumour aged 20. Glio\_0272 was diagnosed with ALL aged 7 months and  
685 was initially treated with chemotherapy, but underwent radiotherapy treatment aged 5 years when the disease  
686 recurred; they were later diagnosed with a pedHGG\_RTK1C tumour. Glio\_0224 was treated with radiotherapy  
687 for ALL aged 2 years, and then diagnosed with a tumour classifying as a PXA. An NOS case (0.22 scoring  
688 GBM\_CBM, Glio\_0218) was treated for a desmoplastic medulloblastoma as a child with chemotherapy and  
689 radiotherapy, and subsequently diagnosed with an HGG aged 20. HGG\_E cases showed a worse overall survival  
690 when compared to pedHGG\_RTK1A and pedHGG\_RTK1B cases in the cohort (median OS survival of 7.9,  
691 16.0 and 16.0 months respectively) (**figure 6F**).

692

693 Multivariate analyses show that the pedHGG\_RT1B and HGG\_E methylation classes were associated with poor  
694 survival (hazard ratio 1.69 (0.827-5)  $p=0.15$  and 3.53 (2.26-13.4)  $p=0.041$  respectively) (**supplementary figure**  
695 **6A**). The GBM\_MES\_ATYP methylation subclass also was significantly associated with poor outcomes (3.86  
696 (2.47-14.6)  $p=0.03$ ). Mutations in *SETD2* and *MET* were also associated with worse survival compared to  
697 wildtype cases (hazard ratios 2.02 (1.03-6.12)  $p=0.07$  and 2.19 (1.41-8.33)  $p=0.18$  respectively)  
698 (**supplementary figure 6B**). Amplifications in *MET*, *CDK4*, *MYCN* and *PDGFRA* were associated with worse  
699 survival, whereas *CDKN2A/B* deletions did not impact survival (**supplementary figure 6C**). GTR with

700 adjuvant chemotherapy alone was significantly associated with worse outcomes (hazard ratio 4.26 (2.92-17.8)  
701  $p=0.03$ ), as was the decision to undertake a biopsy rather than a resection (hazard ratio 2.63 (1.42-8.33)  
702  $p=0.026$ ) (**supplementary figure 6D**). *PDGFRA* and *TP53* mutations were significantly associated with a worse  
703 overall survival within the TYA cohort compared to wildtype cases (hazard ratios 3.36 (1.96-11.4)  $p=0.014$ , and  
704 2.07 (0.922-5.8)  $p=0.013$  respectively) (**supplementary figure 6B,E,F**). However, in many cases throughout  
705 these analyses, the numbers are small and therefore these results should be treated with caution.

706  
707  
708  
709  
710  
711  
712  
713  
714  
715  
716  
717  
718  
719  
720

## 721 **Discussion**

722  
723  
724  
725  
726  
727  
728  
729

TYA HGGs are a diverse group of tumours, sharing many clinical challenges of HGGs occurring in other age groups. The limited research in this age group, with few studies and limited molecular data currently available has further impacted on management (15). The current study investigated a large international multi-institutional cohort of TYA HGG to provide greater insights into their spectrum. An integrated approach to tumour classification and characterisation, using DNA methylation profiling, fusion panel, WES, and histological review highlighted the importance of this approach when adopted in diagnosis and tumour stratification (26).

730  
731  
732  
733  
734  
735  
736  
737  
738  
739

In the UK and Europe, the age definition of TYA is (15-24 years) (27). The WHO classification recognises that there are adult-type and paediatric-type HGGs, but that these tumours can occur outside of these predicted profiles. The rationale to use the age range of 13-30 years was to explore whether there were specific tumour types with a median incidence occurring within the TYA window, but also to explore the possible tails of distribution beyond the classic age limit; pedHGG\_A (median age 13.8), HGG\_E (median age 15.8), pedHGG\_RTK1A/1B/1C (median ages 16.6, 16.6, 22.4 respectively), pedHGG\_RTK2B (median age 19.7), and PXA (median age 17.3) all had a median ages within the 13-30 window. Although the median age for the HGG\_B group was 35.1 years, the age density peak was 29.5 years; the MNP classifier currently defines this as an ‘adult-type diffuse high-grade glioma, IDH-wildtype tumour’ but our study highlights that this may not be the case, and that it may correlate more closely with other paediatric-type subgroups or be a true TYA subgroup.

740 With the acquisition of additional methylation data for GBM\_CBM and GBM\_MES\_ATYP cases, irrespective  
741 of age, their median ages were 36.8 and 50.4 years respectively. However, despite this not being a population-  
742 based study, GBM\_CBM shows a long tail of distribution extending into older adults, and the  
743 GBM\_MES\_ATYP shows a bimodal distribution, including the TYA window. The age-density plots for  
744 different HGG subgroups in this study highlight that age is important, but not an arbitrary singular cut-off; it  
745 should be more appropriately defined by distribution medians and confidence intervals. Broad age inclusion  
746 criteria (or no age exclusions) will be helpful to consider in future studies; HGG subtype-specific studies could  
747 focus on identifying cases via their molecular characteristics, rather than an age definition. Comparative studies  
748 with other published cohorts will therefore require the prioritisation of molecular profiling (including the use of  
749 DNA methylation profiling), opposed to comparative age inclusion criteria.

750  
751 Within this study, we accepted an MNP12 calibrated score of  $>0.5$  as acceptable for classification. The use of  
752 scores  $>0.9$  in Capper *et al* 2018 as well as the MNP website is a conservative threshold (8). For example, if a  
753 calibrated score of  $>0.9$  is not achievable, the classifier can still assign the case to a glioma family group. Also,  
754 tumour classification was undertaken by integrating MNP classifier outputs, sequencing data, and clinical  
755 information, utilising the integrated approach used in neuropathology diagnostic setting. It is also important to  
756 consider the context of this study which is an exploratory research project, helping to refine future diagnostic  
757 practice. Therefore, the need for diagnostic precision, where the output will influence treatment in individual  
758 cases, is not the goal. A calibrated score of  $<0.9$  should not automatically mean that the class assignment is not  
759 of value (9); many factors can influence the score including the cellularity, tumour percentage and the presence  
760 of necrosis. However, if the assignment is still comparable with the histological features or other sequencing  
761 results (which provide a further level of scrutiny), then this can still support the diagnosis. The copy number  
762 data derived from the Illumina array data is also very valuable, illustrating characteristic copy number changes  
763 which can either support or refute the suggestion by the classifier, or the neuropathologist's suspicions. If  
764 genomics data, copy number changes, histological features, and the t-SNE position align, the inclusion of cases  
765 with a score  $<0.9$  was justified.

766  
767 Rare subgroups showed a peak age distribution in the TYA age group (GBM\_CBM, GBM\_MES\_ATYP,  
768 HGG\_B) compared to paediatric ( $<13$ ) and adult ( $>30$ ) ages. Distinct patterns of copy number are seen between  
769 all three of these subgroups when comparing data from tumours occurring in those aged  $<30$  vs  $>30$  years, most  
770 prominently with the GBM\_MES\_ATYP group. At this stage, methylation does not seem to suggest that those  
771 occurring in patients aged  $<30$  are a different subgroup, but further sequencing data and clinical annotations are  
772 needed to explore if the distinctions in copy number represent a solitary molecular difference.

773  
774 The GBM\_CBM group are currently defined by the methylation classifier as occurring in the cerebellum. Early  
775 studies on cerebellar glioblastoma showed that they were seen more frequently in younger patients with a  
776 median age of 52 years (range 5-88 years) and classified predominantly as anaplastic astrocytoma with piloid  
777 features (now known as HGAP) and the former GBM\_MID methylation class, with the tumours demonstrating  
778 similar methylation profiles to DMG\_K27 tumours, but with an absence of the histone mutation (28). However,  
779 there are other methylation subgroups which are found in this location but of lower frequency, including

780 GBM\_MES, GBM\_RTK1 and GBM\_RTK2, leading authors to suggest that they don't represent a molecularly  
781 uniform tumour (28). However, our study suggests otherwise, that there is in fact a distinct methylation  
782 subgroup, with a peak of distribution in the TYA window, and some potentially occurring post-radiotherapy  
783 after treatment for medulloblastoma in childhood. Interestingly, despite implications of current terminology in  
784 the classifier, they do not occur exclusively in the cerebellum.

785  
786 The HGG\_B group appear to be the only true TYA subgroup identified within this study, and there are currently  
787 no published studies focussed on this subgroup. They can occur in hemispheric, midline and posterior fossa  
788 locations, and display a variable copy number profile, with some changes more specific to those patients aged  
789 <30. Alongside frequent *TP53* alterations and variable incidences of *CDKN2A/B* deletions, *BCOR* alterations,  
790 amplifications across different genes including *MYCN*, *MET* and *CDK4* appear to be a characteristic feature.  
791 Histologically, they showed variable appearances, but a proportion were noted to be associated with  
792 microcalcifications. Therefore, DNA methylation profiling remains the crucial molecular test for diagnosis.  
793 Larger cohort studies including *in vitro* and *in vivo* work are needed to further explore targetable associations.

794  
795 Although clinical annotations were incomplete, there is a suggestion of better survival in some paediatric-type  
796 subgroups including pedHGG\_RTK1A, but more data is needed to validate this trend. There are several tumour  
797 predisposition syndromes associated with HGGs including CMMRD and Li Fraumeni (29,30), and this study  
798 identified several incidences of these. Tumours which occur as a result of DNA replication-repair deficiency  
799 contain pathogenic variants in polymerase-proofreading genes and/or mismatch repair genes (31). Existing  
800 studies report a median age of 50 years (range 27-78), an association with the histological giant cell variant of  
801 GBM, and most frequently classifying as the pedHGG\_RTK1A methylation group (32). They contain high  
802 mutation and microsatellite burdens, but their association with high T-cell infiltration leads to the optional use of  
803 immune checkpoint inhibition; synergistic combinations (the addition of ipilimumab and the use of MEK-  
804 inhibition) have shown promise in those where immune checkpoint inhibition does not work (33,34). In one  
805 study, 4/5 cases classifying as pedHGG\_RTK1A and treated with immune check point blockage survived  
806 greater than 3 years, and there was an overall survival of 36.8 months compared to 15.5 months for other HGGs  
807 in the study (32). Hypermutation can also be induced by temozolomide treatment in both IDH-mutant and IDH-  
808 wildtype LGG and HGG (31,35), which is an important consideration for tumours that may have undergone  
809 transformation to a higher-grade glioma, and the potential value of longitudinal sampling to monitor molecular  
810 changes as treatment progresses. One such case in our cohort of a tectal plate pilocytic astrocytoma which was  
811 treated with radiotherapy and years later was diagnosed with an HGG is a case in point. Similarly, we report  
812 siblings with CMMRD; novel homozygous *MSH6* mutations have been previously reported in siblings, and  
813 resulted in an HGG and T-ALL in an 11-year-old female, and a GBM in her 10-year-old brother, both of which  
814 rapidly progressed (36).

815  
816 Ionising radiation is the only known risk factor for the development of a secondary HGG, but the incidence is  
817 only at 1% (37,38), with variable latency periods seen across all age spectrums (39). A striking feature of our  
818 cohort was that 8.6% of cases had been treated for a childhood malignancy (most frequently ALL or a  
819 medulloblastoma of the cerebellum), with a subsequent HGG diagnosis in their adolescent years. The risk that

820 previous radiation poses for the development of HGGs has been reported in the literature (39–42), and it is  
821 important to recognise that these secondary tumours occur in the TYA population, classifying as primarily  
822 pedHGG\_RTK1B or HGG\_E subgroups in our cohort. Existing studies also show that these tumours cluster  
823 with the pedHGG\_RTK1 subgroups, and are associated with *PDGFRA* and *CDK4* gains and losses of  
824 *CDKN2A/B* and *BCOR* (42). Transcriptome analysis has also identified two subgroups (stem-like and pro-  
825 inflammatory), with drug assays suggesting that protease inhibitors may be effective in the pro-inflammatory  
826 subgroup (42). It highlights the need for further studies of these biological and molecular alterations, occurring  
827 at the time of, and post-treatment. Better risk stratification is also needed for those most vulnerable and earlier  
828 identification for patients who have been treated for a childhood cancer (including non-CNS tumours),  
829 potentially with the use of screening during their TYA years. Avoiding the harmful use of radiotherapy to treat  
830 childhood cancers should be the goal (43).

831  
832 A cohort of 207 cases represents one of the largest cohorts of TYA cases published in the literature. However, a  
833 limitation of this study is that some of the rarer subgroups identified within this set comprise very small  
834 numbers, and with limited clinical annotations. Where material is available (and after the provision of molecular  
835 testing has been considered), additional immunohistochemical studies may be helpful, particularly for novel  
836 subgroups, and may assist the neuropathologist in identifying these cases at an earlier stage in the diagnostic  
837 workflow, and for those neuropathologists working in lower-middle-income countries. This study also  
838 showcases the value of detailed molecular profiling of all HGG cases, irrespective of age, so that we can  
839 identify examples of these different tumour types which may be occurring outside of their typical or expected  
840 age ranges; this is, and will become, more valuable when further targeted treatments are developed, which are  
841 specific to the alterations we see in these cases. For example, hypermutant cases may be eligible for treatment  
842 with check point inhibitors (44), and the use of *PDGFRA* (45–47) and MAPK-pathway inhibitors (48,49) are  
843 now more established. Other frequently occurring alterations which this study highlights are *CDKN2A/B*  
844 deletions, *PTEN* and *MYCN* alterations; although not specific to HGG, therapies targeting these frequent  
845 changes may help to improve outcomes as part of combination therapies. One of the most significant challenges  
846 with cohort studies is acquiring clinical and survival data. It is important that this data is available in a more  
847 accessible way to researchers to enable direct comparisons between the treatment strategies employed, and to  
848 explore the differences in response. Preclinical studies using patient-derived cell cultures and patient-derived  
849 and cell-line derived xenografts (PDX, CDX) are needed to support this work. Establishing robust  
850 collaborations with local neurosurgical teams will be important for all teams across the neuro-oncology research  
851 network to help meet this urgent need.

852  
853 The development of new molecular tests and the refinement of existing versions is important to consider. For  
854 this study, we have used the most recently updated v12.8 MNP classifier. However, future iterations will be  
855 produced, and alternative classifiers made available, which can lead to differences in assignments between  
856 different versions. It is hoped that the use of allied molecular tests in addition to DNA methylation profiling,  
857 already well established in most centres, will not impact on patient safety or outcomes and maintained the  
858 desired accuracy of diagnosis. It should also be considered that the current version of the classifier is  
859 unpublished, and developed using data which is not entirely publicly available; within this study we have

860 attempted to mitigate these challenges through the direct use of the MNP classifier website (the current classifier  
861 methodology in diagnostic practice), the development of our own reference cohort (using publicly available  
862 data), but also the use of the t-SNE projections and unsupervised clustering as supplementary tools, to visually  
863 see the distribution of the subgroups. Until the eventual publication of the classifier, this remains the most  
864 robust method we have available. The continual development of such evolving platforms must be encouraged  
865 and supported. But it is important for all clinical teams and researchers to be mindful of such changes to see how  
866 existing cohorts are impacted, and whether these changes may be beneficial for TYA HGG patients.

867

## 868 **Conclusion**

869 High-grade gliomas occurring in TYAs, perhaps unsurprisingly, overlap with methylation subgroups in the  
870 paediatric and adult age groups. Some entities cluster within the TYA age group, whilst others display peaks  
871 close to or involving the TYA age range. Novel methylation-defined classes are a feature of TYA HGGs, some  
872 of which show mutational landscapes which may be targetable with immune checkpoint, *PDGFRA* and MAPK-  
873 pathway inhibitors. Neuro-oncologists should be cautious in assigning tumour subgroups as 'adult-type' or  
874 'paediatric-type' as this may influence the level of molecular profiling that will be undertaken in certain clinical  
875 centres in relation to the age of the patient. Patients who have previously been treated for a childhood  
876 malignancy but then develop a secondary HGG, and also backgrounds of tumour predisposition syndromes, are  
877 enriched in the TYA population. DNA methylation profiling, WES/panel sequencing should be performed on  
878 each TYA HGG to accurately diagnose and characterise these complex tumours.

879

880

881

882

## 883 **Funding sources**

- 884 • 2022 - 2024. Starter Grant for Clinical Lecturers. "The classification and characterisation of high-grade  
885 gliomas in teenagers and young adults." 2-year duration. £30,000 over 2 years. Academy of Medical  
886 Sciences.
- 887 • 2022-2024. Clinical Lecturer Support Grant. "The classification and characterisation of high-grade  
888 gliomas in teenagers and young adults." 2-year duration. £100,000 over 2 years. Jean Shanks /  
889 Pathological Society of Great Britain.
- 890 • 2022-2023. Small Grant Scheme. "The classification and characterisation of high-grade gliomas in  
891 teenagers and young adults." 1 year duration. £5000. British Neuropathological Society.
- 892 • 2021-2022. Fergus Scholefield Cancer Research Fund. "The classification and characterisation of high-  
893 grade gliomas in teenagers and young adults." 1 year duration. £5,000. Penguins Against Cancer.

894

## 895 **Acknowledgements**

896 D.H. is supported by funding from the National Institute for Health and Care Research Great Ormond Street  
897 Hospital Biomedical Research Centre. The views expressed are those of the author(s) and not necessarily those  
898 of the National Health Service, the National Institute for Health and Care Research, or the Department of  
899 Health.

900  
901  
902  
903  
904  
905  
906  
907  
908  
909  
910  
911  
912  
913  
914  
915  
916  
917  
918  
919  
920  
921  
922  
923  
924  
925  
926  
927  
928  
929  
930  
931  
932  
933  
934  
935  
936  
937  
938  
939

The Jones Lab is supported by funding from the Royal Marsden Hospital NHS Foundation Trust Biomedical Research Centre, Cancer Research UK, CRIS Cancer Foundation, and the Ollie Young Foundation. The views expressed are those of the author(s) and not necessarily those of the National Health Service, the National Institute for Health and Care Research, or the Department of Health.

Maria Vinci acknowledges Alfredo Cerimele for technical assistance.

## References

1. Guerreiro Stucklin AS, Ryall S, Fukuoka K, Zapotocky M, Lassaletta A, Li C, et al. Alterations in ALK/ROS1/NTRK/MET drive a group of infantile hemispheric gliomas. *Nat Commun.* 2019;10(1):1–13.
2. Clarke M, Mackay A, Ismer B, Pickles JC, Tatevossian RG, Newman S, et al. Infant High-Grade Gliomas Comprise Multiple Subgroups Characterized by Novel Targetable Gene Fusions and Favorable Outcomes. *Cancer Discov.* 2020;10(7):942–63.
3. Ostrom QT, Cioffi G, Gittleman H, Patil N, Waite K, Kruchko C, et al. CBTRUS Statistical Report: Primary Brain and Other Central Nervous System Tumors Diagnosed in the United States in 2012-2016. *Neuro Oncol.* 2019;21:V1–100.
4. Gianni F, Antonelli M, Ferretti E, Massimino M, Arcella A, Giangaspero F. Pediatric high-grade glioma: A heterogeneous group of neoplasms with different molecular drivers. *Glioma.* 2018;1(4):117.
5. Ostrom QT, Cote DJ, Ascha M, Kruchko C, Barnholtz-Sloan JS. Adult glioma incidence and survival by race or ethnicity in the United States from 2000 to 2014. *JAMA Oncol.* 2018;4(9):1254–62.
6. Rong L, Li N, Zhang Z. Emerging therapies for glioblastoma: current state and future directions. *J Exp Clin Cancer Res.* 2022;41(1):1–18.

- 940 7. Pollack IF, Agnihotri S, Broniscer A. Childhood brain tumors: Current management, biological insights,  
941 and future directions. *J Neurosurg Pediatr.* 2019;23(3):261–73.
- 942 8. Capper D, Jones DTW, Sill M, Hovestadt V, Schrimpf D, Sturm D, et al. DNA methylation-based  
943 classification of central nervous system tumours. *Nature.* 2018;555(7697):469–74.
- 944 9. Capper D, Stichel D, Sahm F, Jones DTW, Schrimpf D, Sill M, et al. Practical implementation of DNA  
945 methylation and copy-number-based CNS tumor diagnostics: the Heidelberg experience. *Acta*  
946 *Neuropathol* [Internet]. 2018;136(2):181–210. Available from: [https://doi.org/10.1007/s00401-018-](https://doi.org/10.1007/s00401-018-1879-y)  
947 [1879-y](https://doi.org/10.1007/s00401-018-1879-y)
- 948 10. Drexler R, Brembach F, Sauvigny J, Ricklefs FL, Eckhardt A, Bode H, et al. Unclassifiable CNS tumors  
949 in DNA methylation-based classification: clinical challenges and prognostic impact. *Acta Neuropathol*  
950 *Commun* [Internet]. 2024;12(1):4–11. Available from: <https://doi.org/10.1186/s40478-024-01728-9>
- 951 11. Karimi S, Zuccato JA, Mamatjan Y, Mansouri S, Suppiah S, Nassiri F, et al. The central nervous system  
952 tumor methylation classifier changes neuro-oncology practice for challenging brain tumor diagnoses and  
953 directly impacts patient care. *Clin Epigenetics.* 2019;11(1):1–10.
- 954 12. Louis DN, Perry A, Wesseling P, Brat DJ, Cree IA, Figarella-Branger D, et al. The 2021 WHO  
955 classification of tumors of the central nervous system: A summary. *Neuro Oncol.* 2021;23(8):1231–51.
- 956 13. Gianni F, Giovannoni I, Cafferata B, Diomedi-Camassei F, Minasi S, Barresi S, et al. Paediatric-type  
957 diffuse high-grade gliomas in the 5th CNS WHO Classification. *Pathologica.* 2022;114(6):422–35.
- 958 14. Alken SP, D’Urso P, Saran FH. Managing teenage/young adult (TYA) brain tumors: a UK perspective.  
959 *CNS Oncol.* 2015;4(4):235–46.
- 960 15. Roux A, Pallud J, Saffroy R, Edjlali-Goujon M, Debily MA, Boddaert N, et al. High-grade gliomas in  
961 adolescents and young adults highlight histomolecular differences from their adult and pediatric  
962 counterparts. *Neuro Oncol.* 2020;22(8):1190–202.
- 963 16. Mackay A, Burford A, Carvalho D, Izquierdo E, Fazal-Salom J, Taylor KR, et al. Integrated Molecular  
964 Meta-Analysis of 1,000 Pediatric High-Grade and Diffuse Intrinsic Pontine Glioma. *Cancer Cell.*  
965 2017;32(4):520–537.e5.
- 966 17. Gottardo NG, Gajjar A. Chemotherapy for malignant brain tumors of childhood. *J Child Neurol.*  
967 2008;23(10):1149–59.
- 968 18. Terziev R, Psimaras D, Marie Y, Feuvret L, Berzero G, Jacob J, et al. Cumulative incidence and risk  
969 factors for radiation induced leukoencephalopathy in high grade glioma long term survivors. *Sci Rep*  
970 [Internet]. 2021;11(1):1–9. Available from: <https://doi.org/10.1038/s41598-021-89216-1>
- 971 19. Wu J, Heidelberg RE, Gajjar A. Adolescents and Young Adults With Cancer: CNS Tumors. *J Clin*  
972 *Oncol.* 2024;42(6):686–95.
- 973 20. da Costa MDS, Camargo NC, Dastoli PA, Nicácio JM, Benevides Silva FA, Sucharski Figueiredo ML,  
974 et al. High-grade gliomas in children and adolescents: Is there a role for reoperation? *J Neurosurg*  
975 *Pediatr.* 2021;27(2):160–9.
- 976 21. Mackay A, Burford A, Molinari V, Jones DTW, Izquierdo E, Brouwer-Visser J, et al. Molecular,  
977 Pathological, Radiological, and Immune Profiling of Non-brainstem Pediatric High-Grade Glioma from  
978 the HERBY Phase II Randomized Trial. *Cancer Cell.* 2018;33(5):829–842.e5.
- 979 22. Specialist cancer services for children and young people: Teenage and Young Adults Designated

- 980 Hospitals. 2023.
- 981 23. Nicoll JAR, Bloom T, Clarke A, Boche D, Hilton D. BRAIN UK: Accessing NHS tissue archives for  
982 neuroscience research. *Neuropathol Appl Neurobiol*. 2022;48(2):1–8.
- 983 24. Sturm D, Orr BA, Toprak UH, Hovestadt V, Jones DTW, Capper D, et al. New Brain Tumor Entities  
984 Emerge from Molecular Classification of CNS-PNETs. *Cell*. 2016;164(5):1060–72.
- 985 25. Sturm D, Capper D, Andreiuolo F, Gessi M, Kölsche C, Reinhardt A, et al. Multiomic neuropathology  
986 improves diagnostic accuracy in pediatric neuro-oncology. *Nat Med*. 2023;29(4):917–26.
- 987 26. Gritsch S, Batchelor TT, Gonzalez Castro LN. Diagnostic, therapeutic, and prognostic implications of  
988 the 2021 World Health Organization classification of tumors of the central nervous system. *Cancer*.  
989 2022;128(1):47–58.
- 990 27. Ferrari A, Stark D, Peccatori FA, Fern L, Laurence V, Gaspar N, et al. Adolescents and young adults  
991 (AYA) with cancer: a position paper from the AYA Working Group of the European Society for  
992 Medical Oncology (ESMO) and the European Society for Paediatric Oncology (SIOPE). *ESMO Open*  
993 [Internet]. 2021;6(2):100096. Available from: <https://doi.org/10.1016/j.esmoop.2021.100096>
- 994 28. Reinhardt A, Stichel D, Schrimpf D, Koelsche C, Wefers AK, Ebrahimi A, et al. Tumors diagnosed as  
995 cerebellarglioblastoma comprise distinct molecular entities. *Ann Kathrin Reinhar*. 2019;8:1–12.
- 996 29. Hansford JR, Das A, McGee RB, Nakano Y, Brzezinski J, Scollon SR, et al. Update on Cancer  
997 Predisposition Syndromes and Surveillance Guidelines for Childhood Brain Tumors. *Clin Cancer Res*.  
998 2024;30(11):2342–50.
- 999 30. Michaeli O, Tabori U. Pediatric High Grade Gliomas in the Context of Cancer Predisposition  
1000 Syndromes. *J Korean Neurosurg Soc* [Internet]. 2018 May 1;61(3):319–32. Available from:  
1001 <https://doi.org/10.3340/jkns.2018.0031>
- 1002 31. Choi S, Yu Y, Grimmer MR, Wahl M, Chang SM, Costello JF. Temozolomide-associated  
1003 hypermutation in gliomas. *Neuro Oncol*. 2018;20(10):1300–9.
- 1004 32. Hadad S, Gupta R, Oberheim Bush NA, Taylor JW, Villanueva-Meyer JE, Young JS, et al. “De novo  
1005 replication repair deficient glioblastoma, IDH-wildtype” is a distinct glioblastoma subtype in adults that  
1006 may benefit from immune checkpoint blockade. *Acta Neuropathol* [Internet]. 2024;147(1):1–24.  
1007 Available from: <https://doi.org/10.1007/s00401-023-02654-1>
- 1008 33. Das A, Ercan AB, Tabori U. Neuro-Oncology Advances germline replication-repair deficiency  
1009 syndromes. 2024;6(June):1–6.
- 1010 34. Das A, Fernandez NR, Levine A, Bianchi V, Stengs LK, Chung J, et al. Combined Immunotherapy  
1011 Improves Outcome for Replication-Repair-Deficient (RRD) High-Grade Glioma Failing Anti-PD-1  
1012 Monotherapy: A Report from the International RRD Consortium. *Cancer Discov*. 2024;14(2):259–73.
- 1013 35. Touat M, Li YY, Boynton AN, Spurr LF, Iorgulescu JB, Bohrsen CL, et al. Mechanisms and therapeutic  
1014 implications of hypermutation in gliomas. *Nature* [Internet]. 2020;580(7804):517–23. Available from:  
1015 <http://dx.doi.org/10.1038/s41586-020-2209-9>
- 1016 36. Ilencikova D, Sejnova D, Jindrova J, Babal P. High-grade brain tumors in siblings with biallelic MSH6  
1017 mutations. *Pediatr Blood Cancer*. 2011 Dec;57(6):1067–70.
- 1018 37. Carret AS, Tabori U, Crooks B, Hukin J, Odame I, Johnston DL, et al. Outcome of secondary high-  
1019 grade glioma in children previously treated for a malignant condition: A study of the Canadian Pediatric

- 1020 Brain Tumour Consortium. *Radiother Oncol.* 2006;81(1):33–8.
- 1021 38. Maluf FC, DeAngelis LM, Raizer JJ, Abrey LE. High-grade gliomas in patients with prior systemic  
1022 malignancies. *Cancer.* 2002;94(12):3219–24.
- 1023 39. Deng MY, Sturm D, Pfaff E, Sill M, Stichel D, Balasubramanian GP, et al. Radiation-induced gliomas  
1024 represent H3-/IDH-wild type pediatric gliomas with recurrent PDGFRA amplification and loss of  
1025 CDKN2A/B. *Nat Commun.* 2021;12(1).
- 1026 40. Whitehouse JP, Howlett M, Federico A, Kool M, Endersby R, Gottardo NG. Defining the molecular  
1027 features of radiation-induced glioma: A systematic review and meta-analysis. *Neuro-Oncology Adv.*  
1028 2021;3(1):1–16.
- 1029 41. López GY, Van Ziffle J, Onodera C, Grenert JP, Yeh I, Bastian BC, et al. The genetic landscape of  
1030 gliomas arising after therapeutic radiation. *Acta Neuropathol [Internet].* 2019;137(1):139–50. Available  
1031 from: <https://doi.org/10.1007/s00401-018-1906-z>
- 1032 42. DeSisto J, Lucas JT, Xu K, Donson A, Lin T, Sanford B, et al. Comprehensive molecular  
1033 characterization of pediatric radiation-induced high-grade glioma. *Nat Commun.* 2021;12(1):1–16.
- 1034 43. Jeha S, Pei D, Choi J, Cheng C, Sandlund JT, Coustan-Smith E, et al. Improved CNS control of  
1035 childhood acute lymphoblastic leukemia without cranial irradiation: St Jude Total Therapy Study 16. *J*  
1036 *Clin Oncol.* 2019;37(35):3377–91.
- 1037 44. Bouffet E, Larouche V, Campbell BB, Merico D, De Borja R, Aronson M, et al. Immune checkpoint  
1038 inhibition for hypermutant glioblastoma multiforme resulting from germline biallelic mismatch repair  
1039 deficiency. *J Clin Oncol.* 2016;34(19):2206–11.
- 1040 45. Yang W, Wang S, Zhang X, Sun H, Zhang M, Chen H, et al. New natural compound inhibitors of  
1041 PDGFRA (platelet-derived growth factor receptor  $\alpha$ ) based on computational study for high-grade  
1042 glioma therapy. *Front Neurosci.* 2023;16(January):1–14.
- 1043 46. Lane R, Cilibrasi C, Chen J, Shah K, Messuti E, Mazarakis NK, et al. PDGF-R inhibition induces  
1044 glioblastoma cell differentiation via DUSP1/p38MAPK signalling. *Oncogene.* 2022;41(19):2749–63.
- 1045 47. Paugh BS, Zhu X, Qu C, Endersby R, Diaz AK, Zhang J, et al. Novel oncogenic PDGFRA mutations in  
1046 pediatric high-grade gliomas. *Cancer Res.* 2013;73(20):6219–29.
- 1047 48. Stitzlein LM, Adams JT, Stitzlein EN, Dudley RW, Chandra J. Current and future therapeutic strategies  
1048 for high-grade gliomas leveraging the interplay between epigenetic regulators and kinase signaling  
1049 networks. *J Exp Clin Cancer Res.* 2024;43(1):1–20.
- 1050 49. Izquierdo E, Carvalho DM, Mackay A, Temelso S, Boulton JKR, Pericoli G, et al. DIPG Harbors  
1051 Alterations Targetable by MEK Inhibitors, with Acquired Resistance Mechanisms Overcome by  
1052 Combinatorial Inhibition. *Cancer Discov.* 2022;12(3):712–29.

1053  
1054  
1055  
1056  
1057  
1058  
1059

1060  
1061  
1062  
1063  
1064  
1065  
1066  
1067  
1068  
1069  
1070  
1071  
1072  
1073  
1074  
1075  
1076  
1077  
1078  
1079  
1080  
1081  
1082  
1083  
1084  
1085  
1086  
1087  
1088  
1089  
1090  
1091  
1092  
1093  
1094  
1095  
1096  
1097  
1098  
1099

## Figure Legends

### Figure 1

Defining an intrinsic set of TYA high-grade gliomas. A, Flow diagram providing an overview of the inclusion and exclusion criteria for the assembled cohort of 207 samples from patients aged  $>13 - \leq 30$  years. B, Anatomic location of TYA HGG after exclusion of non-glioma entities by methylation profiling (n = 189). Left, sagittal section showing internal structures; right, external view highlighting cerebral lobes. Each circle represents the proportion of cases occurring in this location, and is coloured by the generic locations for hemispheric (brown), midline (red) and brainstem (pink). C, Pie chart showing the proportion of different methylation subclasses within the cohort, before exclusion of non-glioma entities (n = 195). Each subgroup is represented by a different colour, as indicated by the key. Cases which scored  $<0.5$  using the MNP classifier v12.8 were classed as 'NOS'. 12 cases were excluded based on poor scoring quality control parameters of the methylation data.

### Figure 2

DNA methylation array profiling of the TYA HGG cohort. A, Methylation array profiling and analysis by the Heidelberg classifier excluded 12 cases which failed QC, and identified 34 with a calibrated score of  $<0.5$  which

1100 were assigned as NOS. t-statistic based stochastic neighbour embedding (t-SNE) projection of the remaining  
 1101 158 cases highlighted cohorts which clustered with both adult and paediatric-type HGG subgroups, including  
 1102 some novel methylation-defined subgroups. Cases then underwent further histopathological assessment and in-  
 1103 depth sequencing to either confirm the methylation assignment, or to further characterise the different  
 1104 subgroups. B, t-statistic based stochastic neighbour embedding (t-SNE) projection of the collected cohort of 158  
 1105 TYA cases alone, without the glioma reference set cases. Samples are represented by dots coloured by subtype.  
 1106 C, Age-density plot showing the age distribution and peak incidences of different high-grade glioma subtypes  
 1107 by DNA methylation profiling, comprising 1704 cases derived from the collected TYA cohort and published  
 1108 datasets. Tumours are grouped according to methylation subclasses and predicted age-distribution according to  
 1109 the WHO classification. Dotted lines define the age cut-off for the TYA group in this project (13 and 30 years).

1110

1111 **Figure 3**

1112 DNA copy number profiling of TYA HGG. A, Heatmap representation of segmented DNA copy number for  
 1113 434 cases of TYA glioma profiled on the Illumina 450k EPIC BeadArray platform (dark red, amplification;  
 1114 red, gain; dark blue, deletion; blue, loss). Samples are arranged in columns clustered by contiguous categorical  
 1115 copy number states based upon log ratio thresholds of  $\pm 0.1$  for gain/loss and  $\pm 0.5$  for amplification and deletion,  
 1116 and organised by their DNA methylation subgroups. Clustering used Euclidean distance and a ward algorithm.  
 1117 Methylation annotations are provided as a bar according to the included key. B, Frequency bar plot showing the  
 1118 most frequent amplifications identified from the copy number profiles across the cohort (n=434). C, Frequency  
 1119 bar plot showing the most frequent deletions identified from copy number profiles across the cohort (n=434).

1120

1121 **Figure 4**

1122 Mutations in TYA gliomas. OncoPrint representation of an integrated annotation of single-nucleotide variants,  
 1123 DNA copy-number changes, and structural variants for TYA gliomas (n = 107). Samples are arranged in  
 1124 columns with genes labelled along rows, and are grouped by methylation subclass and landscape of variants.  
 1125 Clinicopathologic and molecular annotations are provided as bars according to the included key.

1126

1127 **Figure 5**

1128 Characterisation of a true TYA HGG subgroup using the collected cohort and publicly available cases with  
 1129 DNA methylation profiling data. A, Gender bar plots showing the gender distribution of the available cases for  
 1130 GBM\_CBM, HGG\_B and GBM\_MES\_ATYP subgroups. B, Violin plots showing the age distribution and  
 1131 median age of the available cases for GBM\_CBM, HGG\_B and GBM\_MES\_ATYP subgroups. C, Anatomic  
 1132 location of poorly-characterised HGG subgroups irrespective of age. Left, sagittal section showing internal  
 1133 structures; right, external view highlighting cerebral lobes. Each circle represents proportion of cases occurring  
 1134 in this location, and is coloured by the tumour subgroups. D, Representative haematoxylin and eosin (H&E)  
 1135 images of the HGG\_B subgroup. E, Kaplan-Meier showing overall survival available by methylation subclass  
 1136 (line colour as per key) for TYA-specific subgroups (n=12). F, Heatmap representation of segmented DNA copy  
 1137 number for the HGG\_B subgroup (dark red, amplification; red, gain; dark blue, deletion; blue, loss). Samples  
 1138 are arranged in columns clustered by contiguous categorical copy number states based upon log ratio thresholds  
 1139 of  $\pm 0.1$  for gain/loss and  $\pm 0.5$  for amplification and deletion. Clustering used Euclidean distance and a ward

1140 algorithm. Methylation annotations are provided as a bar according to the included key. G, OncoPrint  
1141 representation of an integrated annotation of single-nucleotide variants, DNA copy-number changes, and  
1142 structural variants for the HGG\_B subgroup. Samples are arranged in columns with genes labelled along rows,  
1143 and are grouped by methylation subclass. Clinicopathologic and molecular annotations are provided as bars  
1144 according to the included key.

1145

1146 **Figure 6**

1147 Tumour predisposition syndromes and treatment for childhood malignancies within the TYA cohort. A,  
1148 Haematoxylin and eosin (H&E) images showing different cytological and architectural features of the two cases.  
1149 B, t-statistic based stochastic neighbour embedding (t-SNE) projection of selected subgroups from the glioma  
1150 reference cohort. Samples are represented by dots coloured by subtype. The sibling cases are highlighted by the  
1151 black circles and labelled. C, OncoPrint representation of an integrated annotation of single-nucleotide variants,  
1152 DNA copy-number changes, and structural variants for the sibling cases. Samples are arranged in columns with  
1153 genes labelled along rows. Clinicopathologic and molecular annotations are provided as bars according to the  
1154 included key. D, Circos plots demonstrating the hypermutator phenotypes of the sibling cases. Chromosomal  
1155 locations are represented by ideograms arranged around the circle. E, Patient timelines for five patients  
1156 identified within the cohort which were treated for a childhood malignancy. Gender is annotated using symbols  
1157 and a sagittal brain cartoon demonstrates the location of the tumour. A timeline provides details of key events  
1158 throughout the course of treatment. F, Kaplan-Meier showing overall survival available for HGG\_E,  
1159 pedHGG\_RTK1B and pedHGG\_RTK1A cases, (line colour as per key) for the collected cohort (n=34).

1160

1161

**Figure 1**

**A**

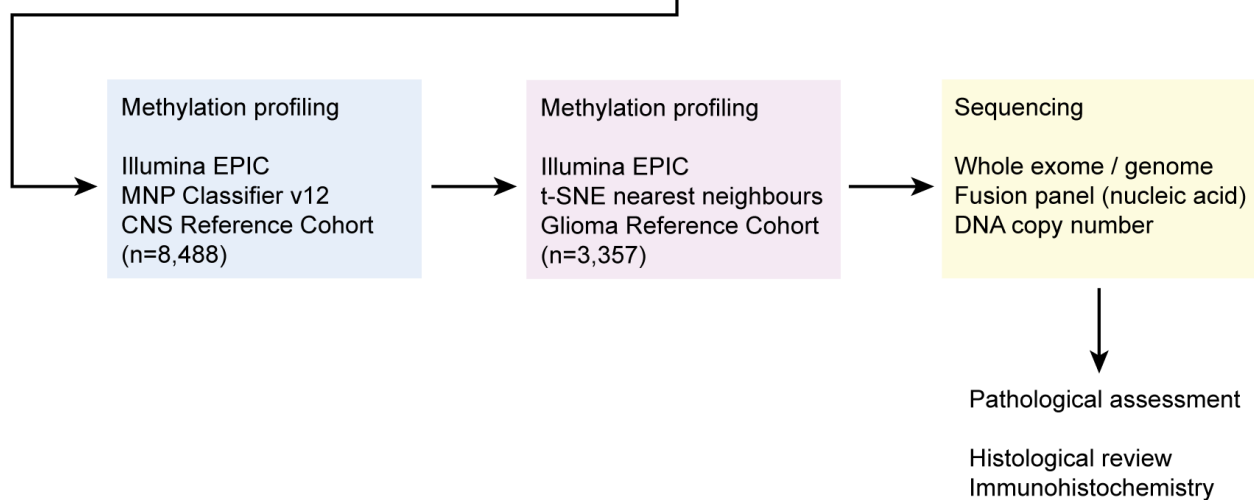
**Inclusions**

13-30 years  
Any CNS locations  
CNS WHO grade 2, 3, 4  
High-grade glioma  
IDH-wildtype, histone-wildtype

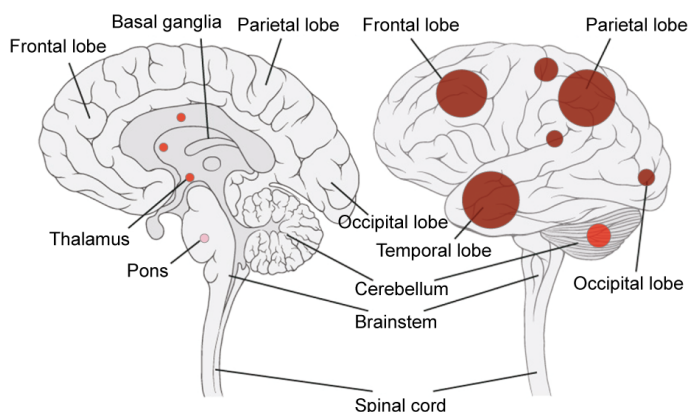
**Exclusions**

Established tumour entities;  
LGG, histone-mutant glioma,  
IDH-mutant glioma, ependymal,  
embryonal, germ cell tumours,  
lymphomas, glioneuronal,  
neuroepithelial tumours

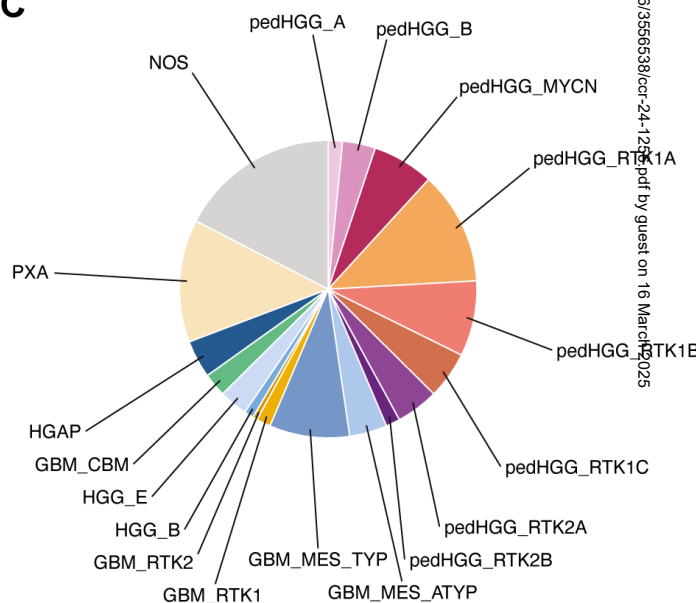
*n*=207

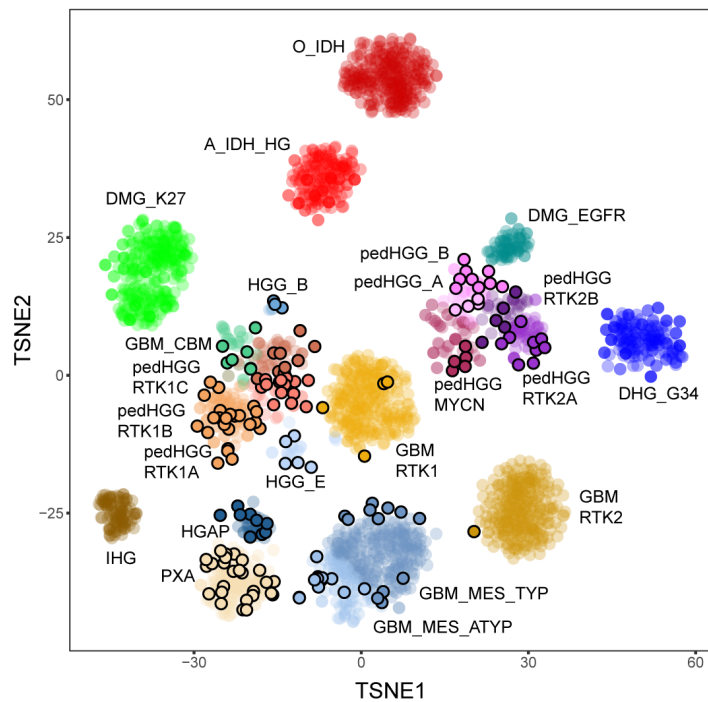
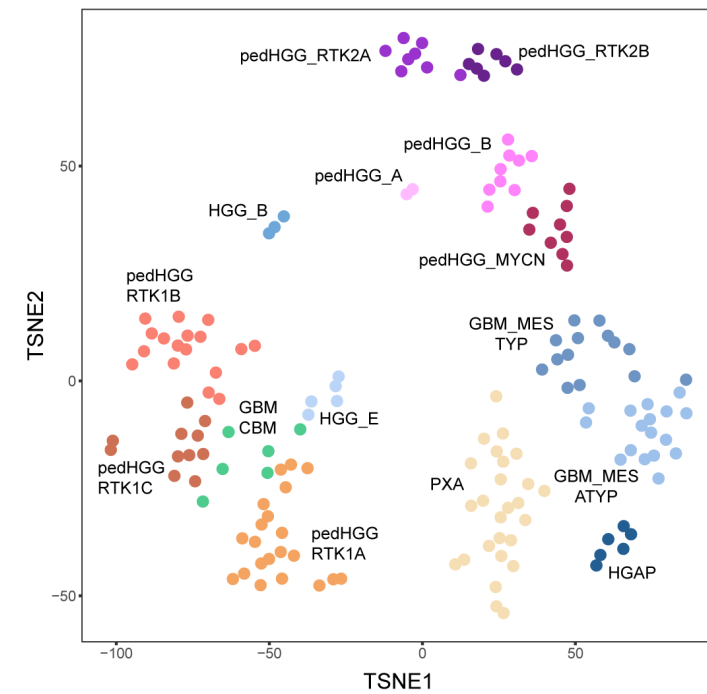
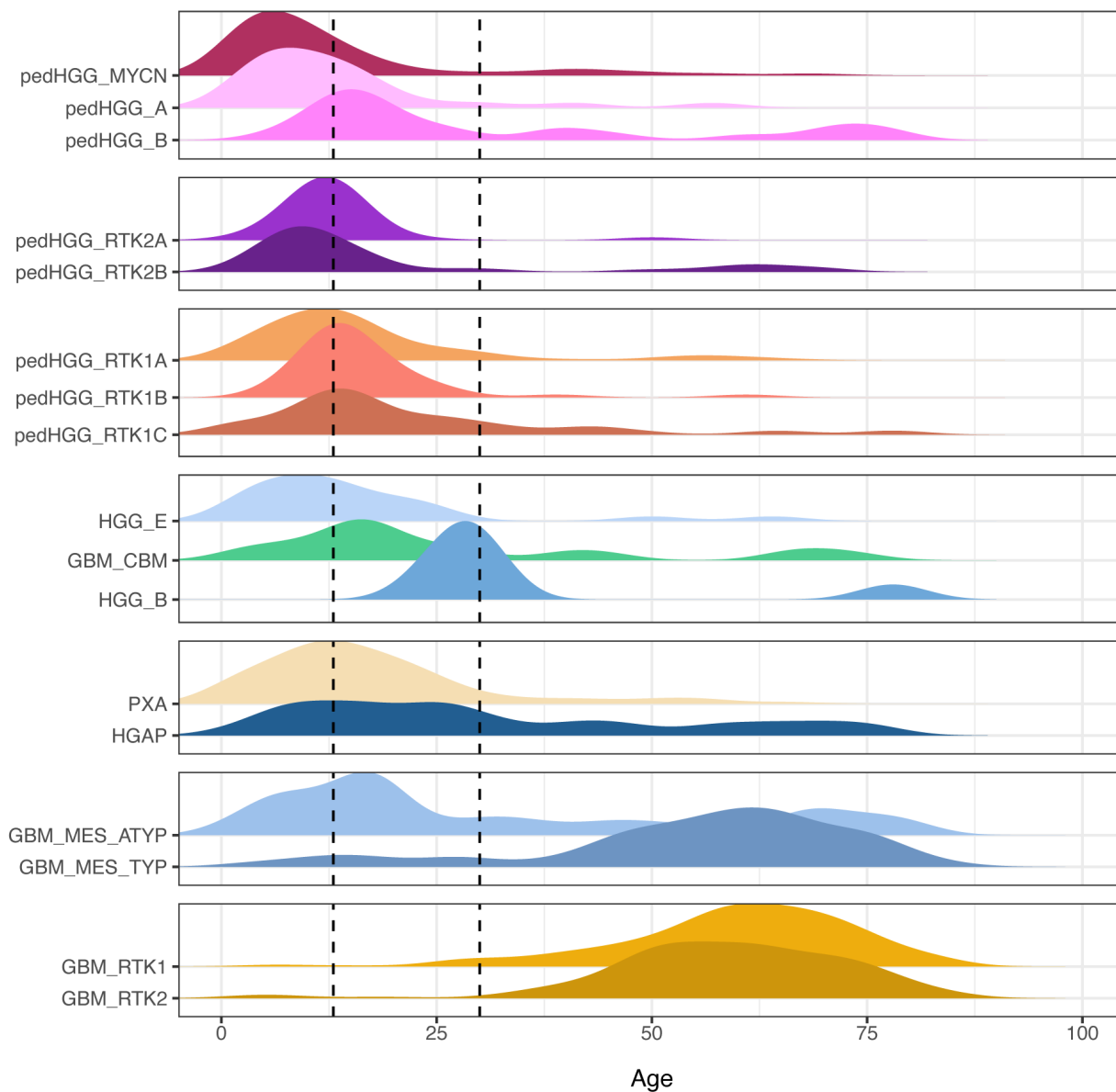


**B**



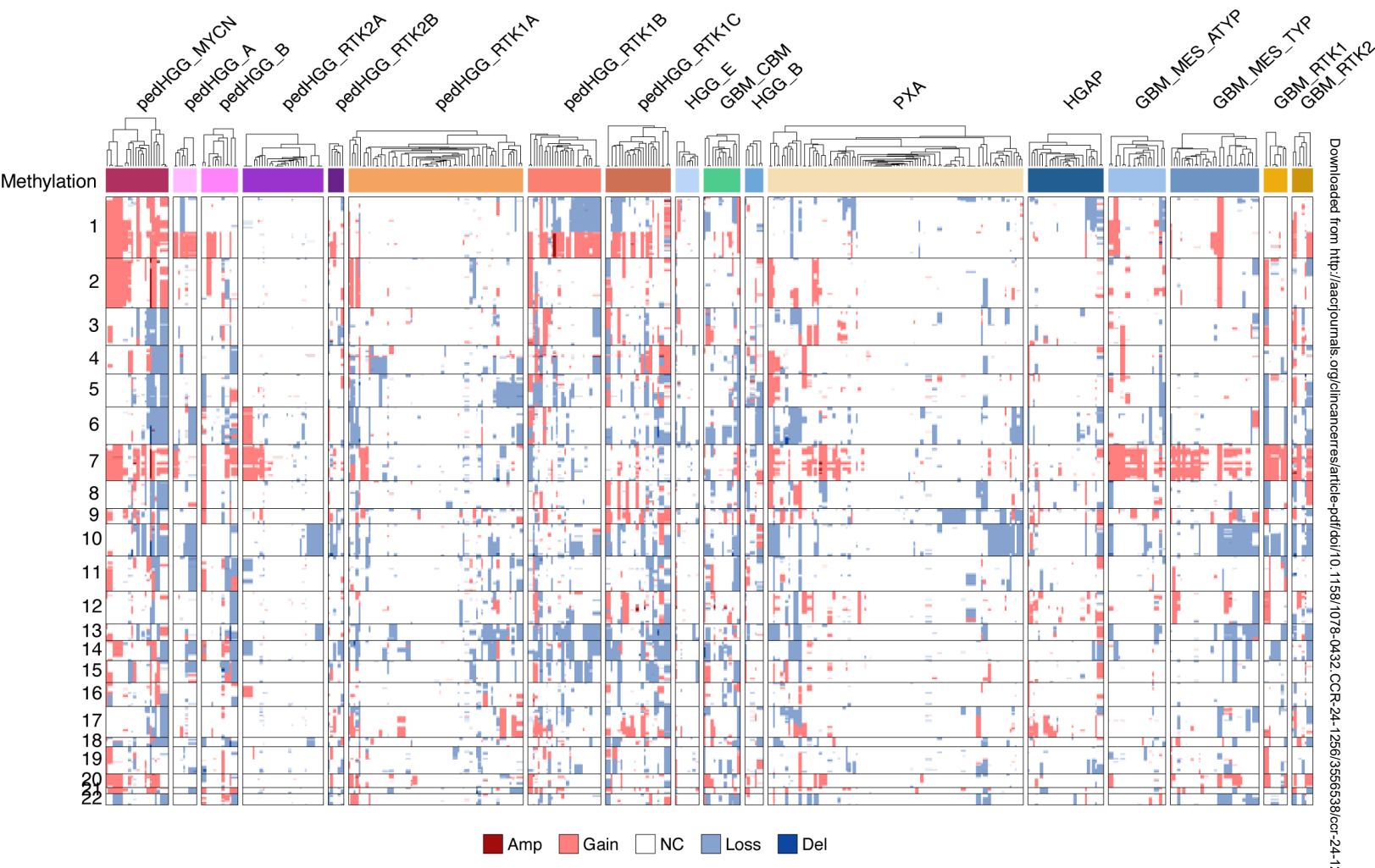
**C**



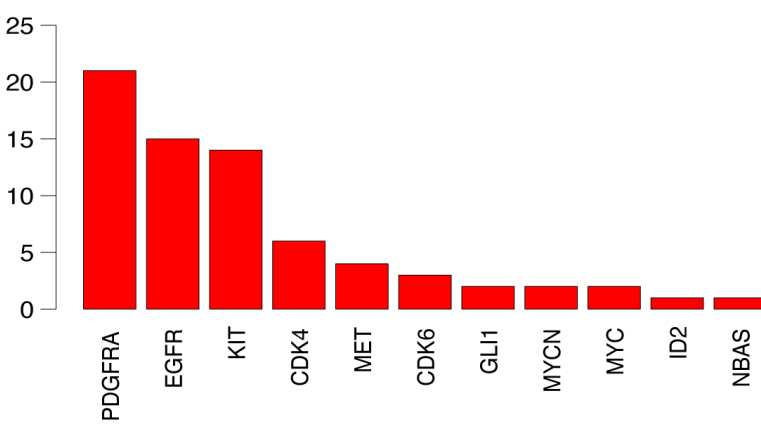
**Figure 2****A****B****C**

**Figure 3**

**A**



**B**



**C**

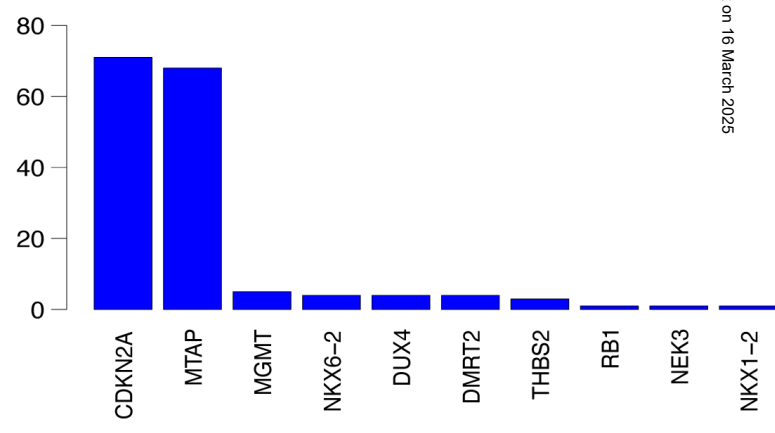


**Figure 4**

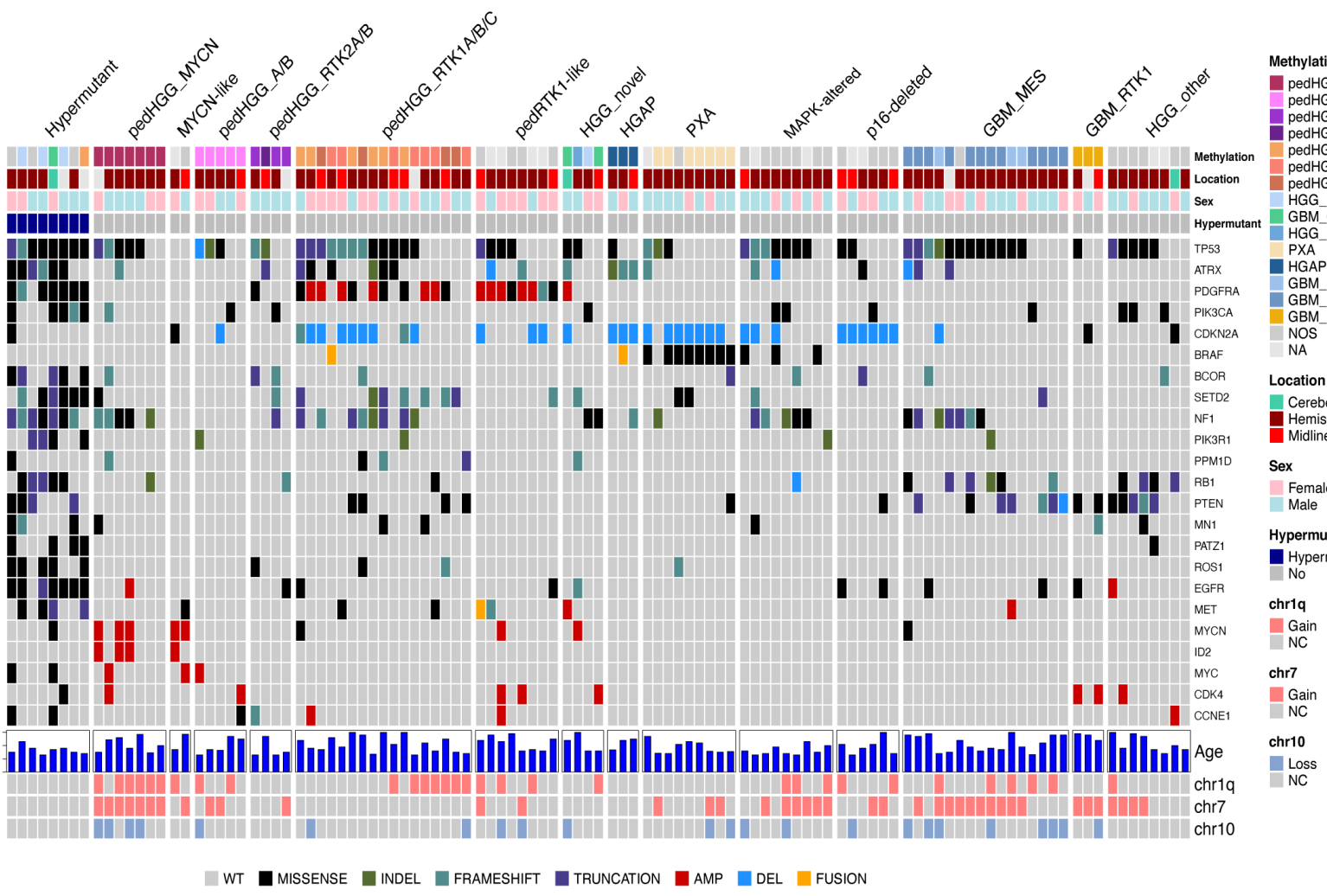


**Figure 5**

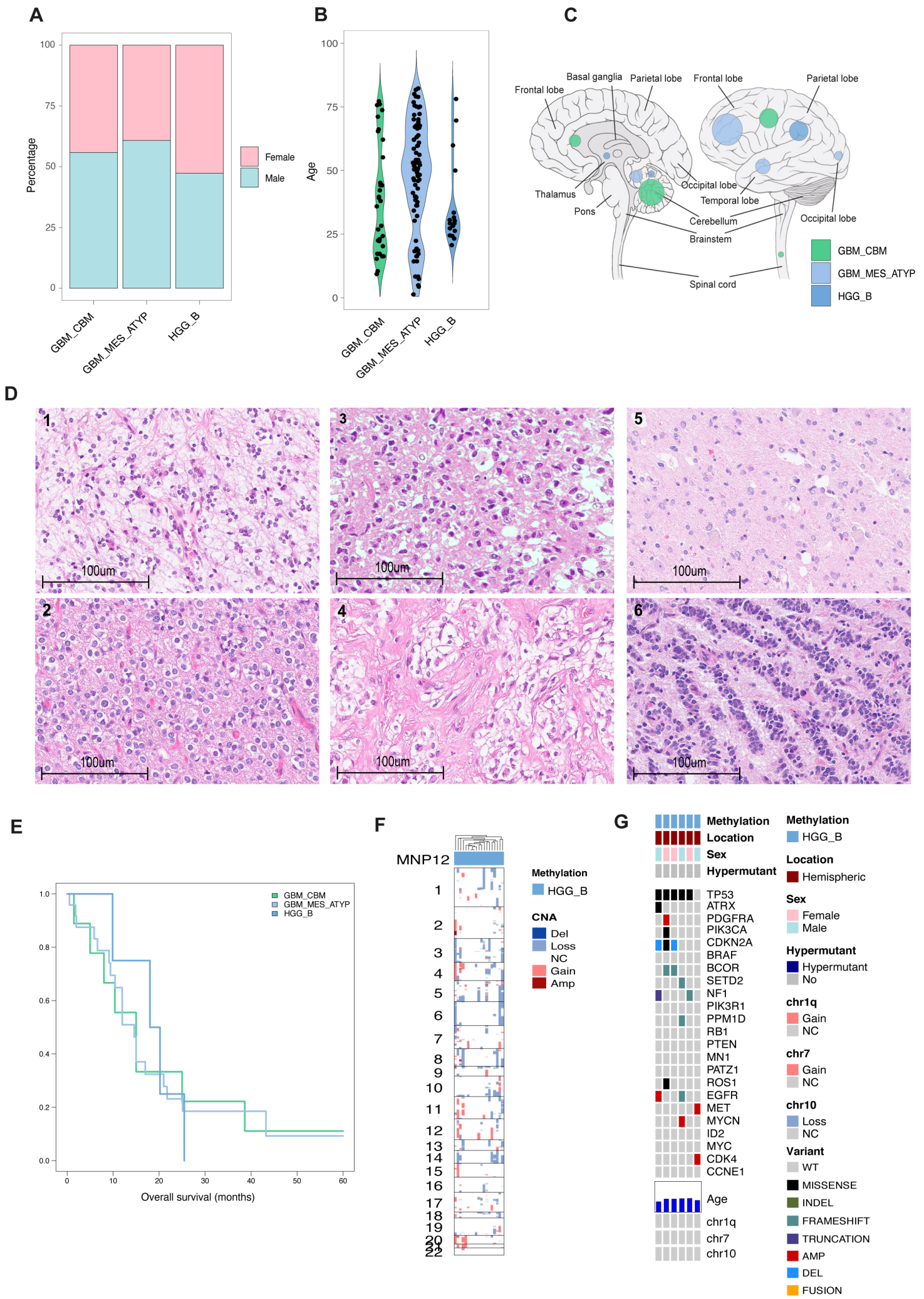
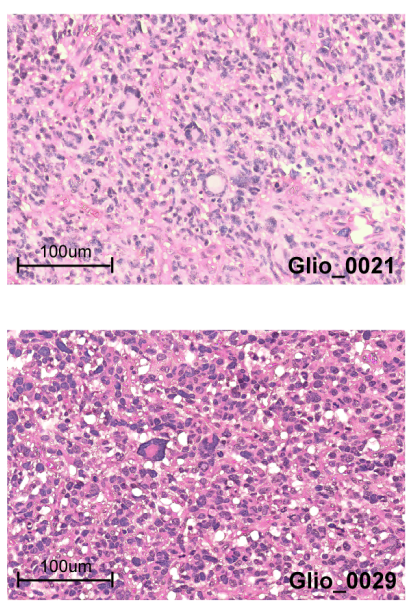
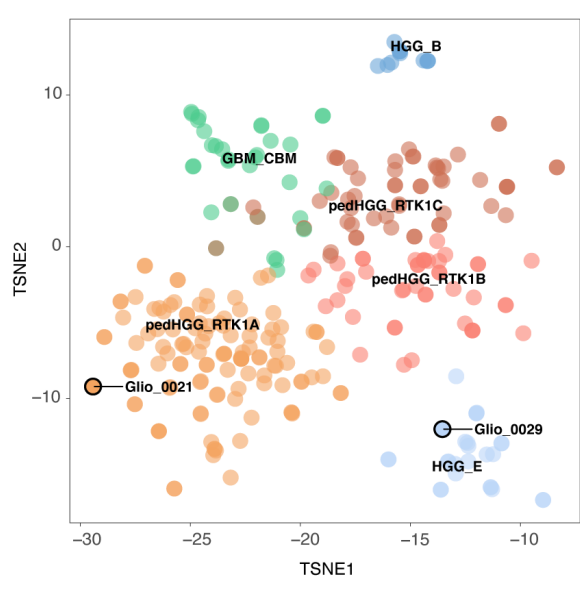


**Figure 6**

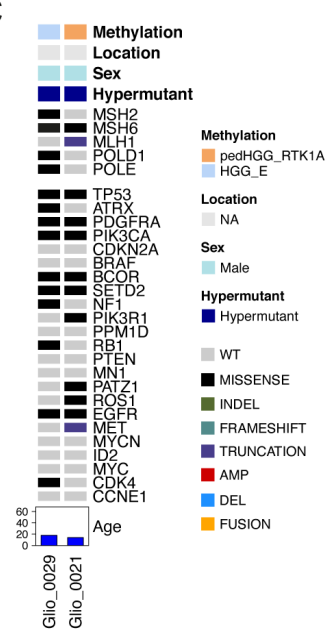
**A**



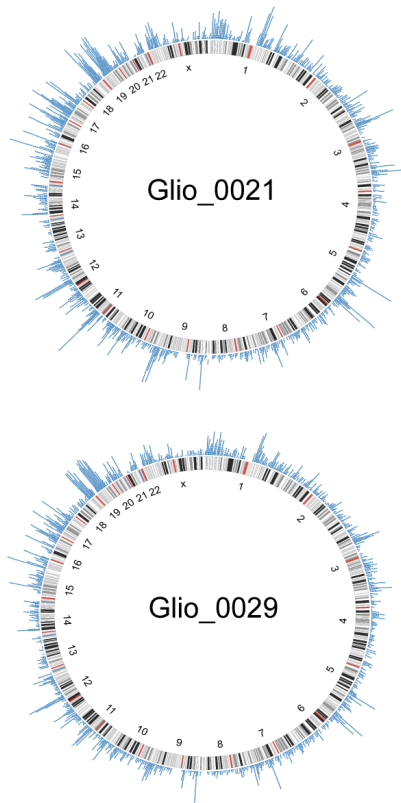
**B**



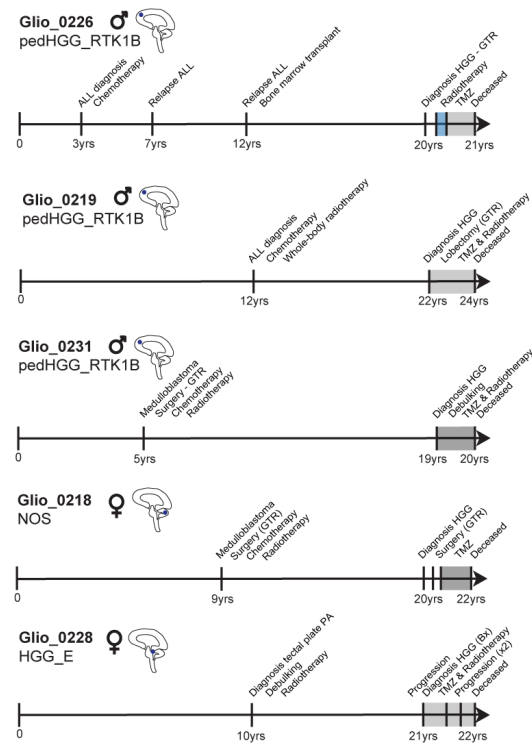
**C**



**D**



**E**



**F**

